

# Science of the Total Environment

## Effect of hydraulic retention time on the electro-bioremediation of nitrate in saline groundwater --Manuscript Draft--

<b>Manuscript Number:</b>	STOTEN-D-22-08067
<b>Article Type:</b>	Research Paper
<b>Section/Category:</b>	
<b>Keywords:</b>	Circular economy; denitrification; microbial electrochemical technology; saline groundwater; value-added products; water recovery
<b>Corresponding Author:</b>	Stefano Milia, Ph.D. National Research Council: Consiglio Nazionale delle Ricerche Cagliari, Cagliari ITALY
<b>First Author:</b>	Giulia Puggioni, Ph.D.
<b>Order of Authors:</b>	Giulia Puggioni, Ph.D. Stefano Milia, Ph.D. Valentina Unali Riccardo Ardu Elena Tamburini Maria Dolores Balaguer Narcis Pous Alessandra Carucci Sebastià Puig
<b>Abstract:</b>	<p>Bioelectrochemical systems (BES) have proven their capability to treat nitrate-contaminated saline groundwater and simultaneously recover value-added chemicals (such as disinfection products) within a circular economy-based approach. In this study, the effect of the hydraulic retention time (HRT) on nitrate and salinity removals, as well as on free chlorine production, was investigated in a 3-compartment BES working in galvanostatic mode, with the perspective of process intensification and future scale-up. Reducing the HRT from <math>30.1 \pm 2.3</math> to <math>2.4 \pm 0.2</math> hours led to a corresponding increase in nitrate removal rates (from <math>17 \pm 1</math> up to <math>131 \pm 1</math> mgNO<sub>3</sub>-N L<sup>-1</sup>d<sup>-1</sup>), although a progressive decrease in desalination efficiency (from <math>77 \pm 13</math> to <math>12 \pm 2\%</math>) was observed. Nitrate concentration and salinity close to threshold limits indicated by the World Health Organization for drinking water, as well as significant chlorine production, were achieved with an optimal HRT of <math>4.9 \pm 0.4</math> h. At the optimal HRT, specific energy consumption was low (<math>6.8 \cdot 10^{-2} \pm 0.3 \cdot 10^{-2}</math> kWh g<sup>-1</sup>NO<sub>3</sub>-Nremoved), considering that the supplied energy supports three processes simultaneously. A logarithmic equation correlated well with nitrate removal rates at the applied HRTs and may be used to predict BES behaviour with different HRTs. The galvanostatic mode exerted a selective pressure on the bacterial community of the cathode biofilm enriching a few dominant populations, including at genus level the taxa Rhizobium, Bosea, Fontibacter and Gordonia. The results provide useful information for the scale-up of BES treating multi-contaminated groundwater.</p>
<b>Suggested Reviewers:</b>	Carolina Cruz Viggi IRSA -CNR: Istituto di ricerca sulle acque Consiglio Nazionale delle Ricerche carolina.cruzvigg@irsa.cnr.it Dr. Cruz Viggi is an expert in bioelectrochemical systems applied to environmental remediation, with several publications on this topic.  Gabriele Beretta Politecnico di Milano gabriele.beretta@polimi.it Dr. Beretta's research is focused on the field of bioelectrochemical systems applied to

	contaminated soil and groundwater remediation
	<p>Xiaofei Wang  Ghent University: Universiteit Gent  Xiaofei.Wang@UGent.be  Dr. Wang is an expert in the field of bioelectrochemical systems applied to water decontamination</p>
	<p>Xiaoting Hong  South China Normal University  hongxt@zstu.edu.cn  Dr Hong's research activities are focused on electrochemistry and electrochemical nitrate removal</p>
	<p>Nicolas Bernet  Senior Researcher, INRAE: Institut National de Recherche pour l'Agriculture l'Alimentation et l'Environnement  nicolas.bernet@inrae.fr  Dr Bernet is an expert in the field of microbial electrochemistry</p>
	<p>Eduard Borrás  Leitat Technological Center: Leitat  eborras@leitat.org  Dr Borrás is an expert in electro bioremediation</p>
<b>Opposed Reviewers:</b>	

Dear Editor,

With the approval of all the Authors, we are submitting the manuscript entitled "*Effect of hydraulic retention time on the electro-bioremediation of nitrate in saline groundwater*" by G. Puggioni, S. Milia, V. Unali, R. Ardu, E. Tamburini, M. Dolors Balaguer, N. Pous, A. Carucci and S. Puig, for its possible publication in Science of the Total Environment.

Nitrate and salinity simultaneously affect groundwater quality in many countries worldwide, hindering the exploitation of such an important water reservoir. Conventional remediation technologies used to remove nitrate and salinity from groundwater are characterized by many technical drawbacks and high operating costs. Our research group recently designed a proof-of-concept based on a 3-compartment bio-electrochemical system (BES) to simultaneously remove nitrates and salinity from groundwater and produce a value-added chemical. The possibility to maximise process performance and push the system toward its limits with the perspective of process scale-up represents a challenging opportunity. Though hydraulic retention time (HRT) is considered a key operating parameter for optimizing hydrodynamics and substrate distribution in conventional BES, its actual role is difficult to be predicted with multi-contaminated groundwater and more complex BES configurations like the one described in this study, where biotic and abiotic processes co-exist in the same reactor. In this study, we investigated how reducing the HRT (i.e., increasing the influent flowrates) may affect process performance in terms of, among the others, nitrate and desalination rates, chlorine production, and energy consumption. We think our results will positively contribute to developing novel, cost-effective, and efficient treatment alternatives based on BES for the remediation of multi-contaminated groundwater, and we consider Science of the Total Environment the ideal platform to share our findings.

We hereby declare that this manuscript represents the original work of the Authors, it has not been published previously, and it won't be submitted for publication elsewhere whilst under consideration by this Journal.

Kind regards,

The Authors.

**Effect of hydraulic retention time on the electro-bioremediation of nitrate  
in saline groundwater**

Giulia Puggioni<sup>1,2</sup>, Stefano Milia<sup>\*,3</sup>, Valentina Unali<sup>3</sup>, Riccardo Ardu<sup>1,4</sup>, Elena Tamburini<sup>4</sup>, M.

Dolors Balaguer<sup>2</sup>, Narcís Pous<sup>2</sup>, Alessandra Carucci<sup>1,3</sup>, Sebastià Puig<sup>2</sup>

<sup>1</sup> University of Cagliari – Department of Civil-Environmental Engineering and Architecture (DICAAR), Via Marengo 2  
- 09123, Cagliari, Italy

<sup>2</sup> Laboratory of Chemical and Environmental Engineering (LEQUiA), Institute of the Environment, University of  
Girona, Carrer Maria Aurelia Capmany, 69, E-17003 Girona, Spain

<sup>3</sup> National Research Council of Italy - Institute of Environmental Geology and Geoengineering (CNR-IGAG), Via  
Marengo 2 - 09123, Cagliari, Italy

<sup>4</sup> DiSB, Department of Biomedical Sciences, University of Cagliari, Cittadella universitaria, 09042 Monserrato (CA),  
Italy

\* Corresponding author:

E-mail address: [stefano.milia@igag.cnr.it](mailto:stefano.milia@igag.cnr.it)

National Research Council of Italy - Institute of Environmental Geology and Geoengineering (CNR-IGAG), Via  
Marengo 2 - 09123, Cagliari, Italy

Tel. +39 070 675 5517, Fax +39 070 675 5523

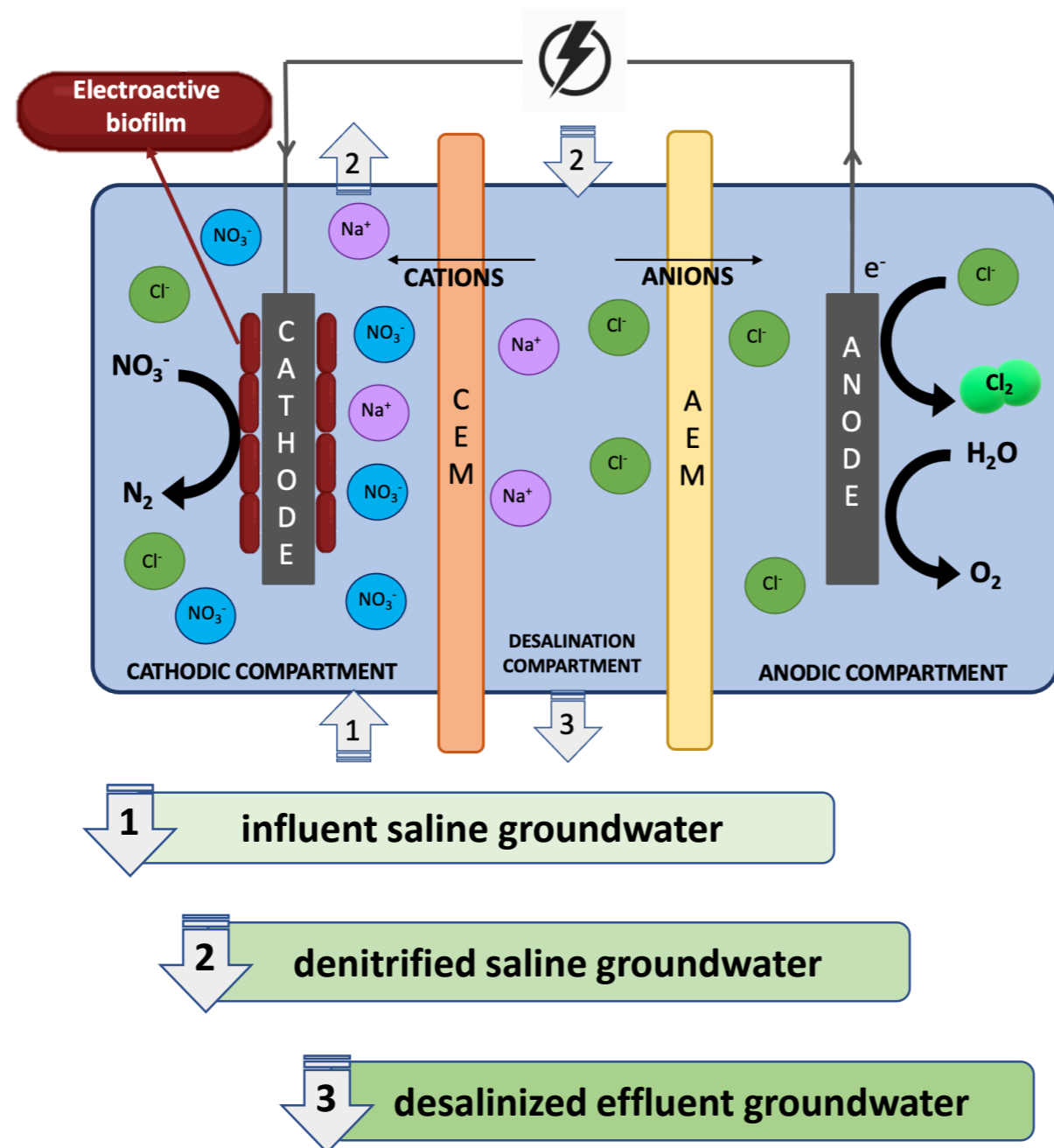
1  
2  
3  
4  
5  
6  
7  
8  
9  
10  
11  
12  
13  
14  
15  
16  
17  
18  
19  
20  
21  
22  
23  
24  
25  
26  
27  
28  
29  
30  
31  
32  
33  
34  
35  
36  
37  
38  
39  
40  
41  
42  
43  
44  
45  
46  
47  
48  
49  
50  
51  
52  
53  
54  
55  
56  
57  
58  
59  
60  
61  
62  
63  
64  
65

### Agro-industrial activities



**Groundwater multi-contamination (nitrate, salinity)**

### Advanced bioelectrochemical systems



**1** influent saline groundwater

**2** denitrified saline groundwater

**3** desalinated effluent groundwater



### Decreasing hydraulic retention time (HRT)

Increasing  $\text{NO}_3^-$  removal rates and efficiency

Stable desalination rates

Decreasing specific energy consumption

Stable  $\text{Cl}_2$  production

Highlights:

- Low HRT improves the nitrate removal performance
- Desalination performance is limited at low HRT
- 3 simultaneous processes are promoted with low energy consumption
- The relationship between nitrate removal rate and HRT follows a logarithmic trend

[Click here to view linked References](#)

# 1                    **Effect of hydraulic retention time on the electro-bioremediation of** 2                    **nitrate in saline groundwater**

3                    Giulia Puggioni<sup>1,2</sup>, Stefano Milia<sup>\*,3</sup>, Valentina Unali<sup>3</sup>, Riccardo Ardu<sup>1,4</sup>, Elena Tamburini<sup>4</sup>,  
4                    M. Dolors Balaguer<sup>2</sup>, Narcís Pous<sup>2</sup>, Alessandra Carucci<sup>1,3</sup>, Sebastià Puig<sup>2</sup>

5                    <sup>1</sup> University of Cagliari – Department of Civil-Environmental Engineering and Architecture (DICAAR), Via  
6                    Marengo 2 - 09123, Cagliari, Italy

7                    <sup>2</sup> Laboratory of Chemical and Environmental Engineering (LEQUiA), Institute of the Environment,  
8                    University of Girona, Carrer Maria Aurelia Capmany, 69, E-17003 Girona, Spain

9                    <sup>3</sup> National Research Council of Italy - Institute of Environmental Geology and Geoengineering (CNR-IGAG),  
10                    Via Marengo 2 - 09123, Cagliari, Italy

11                    <sup>4</sup> DiSB, Department of Biomedical Sciences, University of Cagliari, Cittadella universitaria, 09042  
12                    Monserrato (CA), Italy

13  
14                    \* Corresponding author:

15                    E-mail address: [stefano.milia@igag.cnr.it](mailto:stefano.milia@igag.cnr.it)

16                    National Research Council of Italy - Institute of Environmental Geology and Geoengineering (CNR-IGAG),  
17                    Via Marengo 2 - 09123, Cagliari, Italy

18                    Tel. +39 070 675 5517, Fax +39 070 675 5523

## 19 20                    **Abstract:**

21                    Bioelectrochemical systems (BES) have proven their capability to treat nitrate-contaminated  
22                    saline groundwater and simultaneously recover value-added chemicals (such as disinfection  
23                    products) within a circular economy-based approach. In this study, the effect of the hydraulic  
24                    retention time (HRT) on nitrate and salinity removals, as well as on free chlorine production,  
25                    was investigated in a 3-compartment BES working in galvanostatic mode, with the  
26                    perspective of process intensification and future scale-up. Reducing the HRT from  $30.1 \pm 2.3$   
27                    to  $2.4 \pm 0.2$  hours led to a corresponding increase in nitrate removal rates (from  $17 \pm 1$  up to  
28                     $131 \pm 1$   $\text{mgNO}_3^- \text{-N L}^{-1} \text{d}^{-1}$ ), although a progressive decrease in desalination efficiency (from

29 77±13 to 12±2%) was observed. Nitrate concentration and salinity close to threshold limits  
30 indicated by the World Health Organization for drinking water, as well as significant  
31 chlorine production, were achieved with an optimal HRT of 4.9±0.4 h. At the optimal HRT,  
32 specific energy consumption was low ( $6.8 \cdot 10^{-2} \pm 0.3 \cdot 10^{-2}$  kWh g<sup>-1</sup>NO<sub>3</sub><sup>-</sup>-N<sub>removed</sub>), considering  
33 that the supplied energy supports three processes simultaneously. A logarithmic equation  
34 correlated well with nitrate removal rates at the applied HRTs and may be used to predict  
35 BES behaviour with different HRTs. The galvanostatic mode exerted a selective pressure on  
36 the bacterial community of the cathode biofilm enriching a few dominant populations,  
37 including at genus level the taxa *Rhizobium*, *Bosea*, *Fontibacter* and *Gordonia*. The results  
38 provide useful information for the scale-up of BES treating multi-contaminated  
39 groundwater.

40 **Keywords:** circular economy; denitrification; microbial electrochemical technology; saline  
41 groundwater; value-added products; water recovery.

42

## 43 1. INTRODUCTION

44 Groundwater is a critical freshwater reservoir fundamental for global water and food  
45 security. The spread of contaminants in groundwater can limit its use as drinking water, so  
46 actions must be taken to ensure a safe drinking water supply (Janža, 2022).  
47 Bioelectrochemical systems are emerging as sustainable alternatives for the treatment of  
48 contaminated groundwater. Such systems are based on the ability of electroactive  
49 microorganisms to perform oxidation and reduction reactions by exchanging electrons with  
50 an electrode (Pous et al., 2018; Wang et al., 2020). Therefore, they are particularly suitable  
51 for groundwater treatment, as they promote bioremediation without the supply of chemicals  
52 as electron acceptors/donors.



53 Most of the studies focus on the removal of one type of contaminant at a time (e.g., nitrate,  
54 organics, heavy metals, calcium, etc.), which is useful for a deep understanding and  
55 optimisation of the processes involved (Beretta et al., 2020; Ceballos-Escalera et al., 2022,  
56 2021; Palma et al., 2018; Sevda et al., 2018; Verdini et al., 2015). However, groundwater  
57 matrices are highly complex and heterogeneous, influencing the behaviour of BES and  
58 representing a key aspect of process development and scale-up. One of the most intriguing  
59 challenges that researchers are currently facing is thus the application of BES to the  
60 bioremediation of multi-contaminated groundwater.

61 Among contaminants, nitrate is often found in groundwater at high concentrations co-  
62 existing with other pollutants. Nitrate contamination in groundwater is frequently due to  
63 inefficient farming practices and careless management of livestock activities (Kwon et al.,  
64 2021; Serio et al., 2018). The Nitrates Directive (91/767/EU) sets a nitrate concentration  
65 limit of  $50 \text{ mgNO}_3^- \text{ L}^{-1}$  ( $11.3 \text{ mgNO}_3^- \text{-N L}^{-1}$ ) in drinking water for human health, safety, and  
66 environmental protection. In this framework, the possibility of simultaneously removing  
67 nitrates and other contaminants from groundwater is of particular interest.

68 The presence of co-contaminants associated with nitrate can result from natural sources (e.g.,  
69 arsenic derived from the reductive dissolution of arsenic-rich minerals) and anthropogenic  
70 activities (e.g., perchlorate derived from the production of car airbags, fireworks and  
71 fertilisers, Lian et al., 2016). Ceballos-Escalera et al. (2021) successfully removed nitrate  
72 and arsenic from groundwater using a tubular BES. The treatment combined nitrate  
73 reduction to dinitrogen gas and arsenite oxidation to arsenate (which shows less toxicity,  
74 solubility and mobility) within the same reactor. In this way, the ability of BES to denitrify  
75 without being affected by arsenite and under low electrical conductivity conditions (about 1  
76  $\text{mS cm}^{-1}$ ) was demonstrated.

77 Wang et al., 2021 investigated the simultaneous removal of nitrate and perchlorate from  
78 groundwater with cathodic potential regulation. Results demonstrated that the mechanism of  
79 nitrate and perchlorate reduction in the BES was the direct electron transfer from the cathode  
80 to the bacteria, and the dominant bacterial community on the cathode was proven to have  
81 the ability to reduce nitrate and perchlorate. However, regardless of the potential applied to  
82 the cathode or not, nitrate inhibited the reduction of perchlorate.

83 The occurrence of high nitrate ( $30.0 \text{ mgNO}_3^- \text{-N L}^{-1}$ ) and salinity levels ( $3.3 \pm 0.3 \text{ mS cm}^{-1}$ ) in  
84 groundwater was recently dealt with by Puggioni et al. (2021). In this study, in contrast to  
85 the previous studies where co-contaminants required removal by oxidation/reduction, the  
86 treatment coupled reduction with a separation of co-contaminants. A proof-of-concept based  
87 on a 3-compartment BES allowed the simultaneous removal of nitrate ( $39 \pm 1 \text{ mgNO}_3^- \text{-N L}^{-1}$   
88  $\text{d}^{-1}$ ) and salinity (chloride removal rate of  $13 \pm 2 \text{ gCl}^- \text{ L}^{-1} \text{ d}^{-1}$ ) from groundwater but also the  
89 production of value-added chemicals (i.e., free chlorine). The electroactive biomass attached  
90 to the cathode carried out the denitrification in the bio-cathodic compartment, while  
91 desalination took place in the central compartment thanks to electrochemically driven  
92 migration of ions across the two ion exchange membranes. In the anodic compartment,  
93 anions, mainly chloride, accumulated. Part of the accumulated chloride was converted into  
94 chlorine, which represents a value-added product that could also be used for disinfection in  
95 water treatment plants. The galvanostatic operation (applied current:  $0.16 \text{ mA cm}^{-2}_{\text{membrane}}$ )  
96 with pH control ( $< 9$ ) in the bio-cathodic compartment resulted in high nitrogen and salinity  
97 removal efficiencies ( $69 \pm 2\%$  and  $63 \pm 5\%$ , respectively) and significant recovery of free  
98 chlorine ( $26.8 \pm 3.4 \text{ mgCl}_2 \text{ L}^{-1}$ ). Standard quality requirements for drinking water in terms of  
99 nitrate concentration (91/767/EU) and electrical conductivity (98/83/CE) were successfully  
100 met with this cell configuration. However, considering the high capital costs required to  
101 implement BES-based technologies (Zhang and Angelidaki, 2013) and the need to promote

102 the scale-up of these systems, the process needs to be further optimised by increasing nitrate  
103 removal rates, reducing energy consumption. The performance of such systems could be  
104 limited by the hydrodynamics and the corresponding substrate distribution (Vilà-Rovira et  
105 al., 2015). Hydrodynamics are reinforced at higher flowrates (lower HRTs). This strategy  
106 was confirmed by Ceballos-Escalera et al., 2021 and Pous et al., 2017, reaching higher  
107 denitrifying capacities in denitrifying BES. However, the role of the HRT may be different  
108 in more complex groundwater and BES configurations like the one described by Puggioni  
109 et al. (2021), where biotic (e.g., nitrate removal) and abiotic (i.e., desalination, chloride  
110 removal and chlorine production) processes co-exist in the same reactor. In the present work,  
111 the effects of increasing influent flowrates on simultaneous denitrification and desalination  
112 of groundwater in a 3-compartment cell were investigated, providing helpful information for  
113 its optimisation with a view to a future application at pilot scale. Moreover, the bacterial  
114 communities of biomass established under the galvanostatic mode used in the present study,  
115 and the potentiostatic mode previously tested by Puggioni et al. (2021), were characterised  
116 and compared.

## 117 **2. MATERIALS AND METHODS**

### 118 **2.1 Reactor set-up**

119 Two identical 3-compartment cells made of polycarbonate were used (Puggioni et al., 2021).  
120 The bio-cathode compartment contained the graphite felt cathode electrode (64 cm<sup>2</sup>, degree  
121 of purity 99.9%, AlfaAesar, Germany), and it was physically separated from the central  
122 compartment by a cation exchange membrane (CEM 7000, Membrane International Inc.,  
123 USA). The anode compartment, containing the anode electrode consisting of a titanium mesh  
124 coated with mixed metals oxide (Ti-MMO, 15 cm<sup>2</sup>, NMT-Electrodes, South Africa), was  
125 physically separated from the central compartment by an anion exchange membrane (AEM  
126 7001, Membranes International Inc., USA). A reference electrode (Ag/AgCl, +0.197 V vs  
127 SHE, mod. MF2052, BioAnalytical Systems, USA) was placed in the bio-cathode

128 compartment. Cathode, anode, and reference electrodes were connected to a multichannel  
129 potentiostat (Ivium technologies, IviumNstat, NL). The system was thermostatically  
130 controlled at  $25\pm 1$  °C.

## 131 **2.2 Groundwater characteristics**

132 A synthetic medium mimicking nitrate concentration and salinity of groundwater from the  
133 nitrate vulnerable zone of Arborea (Sardinia, Italy) was fed to the bio-cathode compartment.  
134 This medium contained  $216.6 \text{ mg L}^{-1} \text{ KNO}_3$  (corresponding to  $30.0 \text{ mgNO}_3^{-}\text{-N L}^{-1}$ );  $10 \text{ mg}$   
135  $\text{L}^{-1} \text{ NH}_4\text{Cl}$  (corresponding to  $2.6 \text{ mgNH}_4^{+}\text{-N L}^{-1}$ ),  $4.64 \text{ mg L}^{-1} \text{ KH}_2\text{PO}_4$ ;  $11.52 \text{ mg L}^{-1}$   
136  $\text{K}_2\text{HPO}_4$ ;  $350 \text{ mg L}^{-1} \text{ NaHCO}_3$ ;  $2000 \text{ mg L}^{-1} \text{ NaCl}$  and  $100 \mu\text{L L}^{-1}$  of trace elements solution  
137 (Patil et al., 2010). The media was prepared using distilled water and pre-flushed with  $\text{N}_2$   
138 gas for 15 minutes to avoid any presence of oxygen. The medium's electrical conductivity  
139 and pH were  $3.06\pm 0.5 \text{ mS cm}^{-1}$  and  $8.2\pm 0.3$ , respectively.

## 140 **2.3 Experimental procedure**

141 The cells were started-up and tested as described by Puggioni et al. (2021). The bio-cathode  
142 compartment was continuously fed with groundwater, and the effluent was sent into the  
143 central compartment to achieve desalination. Tap water was recirculated in the anode  
144 compartment and replaced periodically (about every 10 days). The potentiostat was set in  
145 galvanostatic mode at current of  $10 \text{ mA}$  ( $0.16 \text{ mA cm}^{-2}_{\text{membrane}}$ ). A pH control ( $< 9$ ) was  
146 implemented to avoid excessive pH increases in the bio-cathode compartment by dosing HCl  
147 ( $1 \text{ M}$ ) in the bio-cathode recirculation line. The probe for continuous pH measurement  
148 (Mettler Toledo, mod. InPro 3253i/SG/225, USA) was connected to a transmitter (Mettler  
149 Toledo, mod. M300, USA), which recorded data every 10 minutes.

150 The enhancement of electro-bioremediation systems must be linked to the treatment  
151 capacity. In this sense, hydraulic retention time (HRT) was used as the operational  
152 parameter, as presented in Table 1.

153 Different HRTs were tested, from the previous proof-of-concept (Puggioni et al. 2021) value  
 154 30.1±2.3 (Test 1) to 2.4±0.2 h (Test 6), by increasing the influent flowrate. During Test 7,  
 155 the same HRT of Test 5 (4.9±0.4 h) was applied to confirm the stability of the system. Each  
 156 HRT was maintained for about one month. The nitrate concentration in the influent was also  
 157 maintained at 29.3±3.5 mgNO<sub>3</sub><sup>-</sup>-N L<sup>-1</sup>.

158 Table 1. Experimental procedure.

Tests	Influent flowrate [L d <sup>-1</sup> ]	HRT Bio-cathode + central compartment [h]	HRT' central compartment [h]	NO <sub>3</sub> <sup>-</sup> -N loading rate [mg L <sup>-1</sup> d <sup>-1</sup> ]
1	0.11	30.1±2.3	6.7±0.3	23.57±1.84
2	0.17	20.3±1.5	4.5±0.2	35.14±2.39
3	0.31	10.9±0.8	2.4±0.1	62.61±3.90
4	0.46	7.3±0.6	1.6±0.1	82.21±3.07
5	0.68	4.9±0.4	1.1±0.05	125.48±2.98
6	1.42	2.4±0.2	0.5±0.02	261.05±16.07
7	0.68	4.9±0.4	1.1±0.05	130.92±11.27

159

## 160 2.4 Analytical methods

161 Samples were periodically drawn from influent (once per week), effluent (three times per  
 162 week), bio-cathode and anode compartments (three times per week) in order to evaluate  
 163 overall cell performances. The same samples from the duplicate cell were taken once a week  
 164 to confirm the process progress of the main cell. Liquid samples were analysed for  
 165 quantification of anions, i.e., chloride (Cl<sup>-</sup>), nitrite (NO<sub>2</sub><sup>-</sup>-N), nitrate (NO<sub>3</sub><sup>-</sup>-N), phosphate  
 166 (PO<sub>4</sub><sup>3-</sup>), and sulphate (SO<sub>4</sub><sup>2-</sup>), using an ion chromatograph (ICS-90, Dionex-ThermoFisher,  
 167 USA) equipped with an AS14A Ion-PAC 5 µm column. Samples were filtered (acetate  
 168 membrane filter, 0.45 µm porosity) and properly diluted with grade II water. The  
 169 concentrations of the main cations, i.e., potassium (K<sup>+</sup>) and sodium (Na<sup>+</sup>), were determined

170 using an ICP/OES (Varian 710-ES, Agilent Technologies, USA): samples were filtered  
171 (acetate membrane filter, 0.45 µm porosity), acidified (nitric acid, 1% v:v) and diluted with  
172 grade I water.

173 Electrical conductivity and pH were measured using a benchtop meter (HI5522, Hanna  
174 Instruments, Italy).

175 The concentration of free chlorine was analysed using spectrophotometric techniques  
176 (DR1900, Hach Lange, Germany) and the DPD (N,N-diethyl-p-phenylenediamine) free  
177 chlorine method (DPD free chlorine reagent powder pillows Cat. 2105569, Hach Lange,  
178 Germany).

179 Nitrous oxide (N<sub>2</sub>O) was measured using an N<sub>2</sub>O liquid-phase microsensor (Unisense, Den-  
180 mark) located in the effluent line of the reactors, thanks to a dedicated glass measuring cell.

181 The resulting bio-cathode potentials were recorded every five minutes through potentiostat  
182 (Ivium technologies, IviumNstat, NL). Cell potential was periodically checked using a  
183 multimeter (K2M, mod. KDM-600C, Italy).

## 184 **2.5 Calculations**

185 Nitrate Removal Efficiency (N-RE) and Nitrate Removal Rate (N-RR) were calculated  
186 according to equations 1 and 2, respectively:

$$187 \quad N - RE [\%] = \frac{C_{NO_3^- - N(inf)} - C_{NO_3^- - N(eff)}}{C_{NO_3^- - N(inf)}} \times 100 \quad (1)$$

$$188 \quad N - RR [mg \ N \ L^{-1} \ d^{-1}] = \frac{C_{NO_3^- - N(inf)} - C_{NO_3^- - N(eff)}}{HRT} \quad (2)$$

189 Where  $C_{NO_3^- - N(inf)}$  and  $C_{NO_3^- - N(eff)}$  [mgNO<sub>3</sub><sup>-</sup>-N L<sup>-1</sup>] are nitrate concentrations in the influent  
190 and the effluent, respectively, while HRT [d] is the hydraulic retention time considering the  
191 volumes of the cathodic and central compartments.

192 The desalination performance was evaluated by calculating the electrical conductivity  
193 removal efficiency (EC-RE, equation 3), the chloride removal efficiency (Cl<sup>-</sup>-RE, equation  
194 4), and the chloride removal rate (Cl<sup>-</sup>-RR, equation 5).

$$195 \quad EC - RE [\%] = \frac{EC_{(inf)} - EC_{(eff)}}{EC_{(inf)}} \times 100 \quad (3)$$

$$196 \quad Cl^- - RE [\%] = \frac{C_{Cl^- (inf)} - C_{Cl^- (eff)}}{C_{Cl^- (inf)}} \times 100 \quad (4)$$

$$197 \quad Cl^- - RR [mg L^{-1} d^{-1}] = \frac{C_{Cl^- (inf)} - C_{Cl^- (eff)}}{HRT'} \quad (5)$$

198 where  $EC_{(eff)}$  [ $mS cm^{-1}$ ] and  $C_{Cl-(eff)}$  [ $mg L^{-1}$ ] represent the effluent electrical conductivity and  
 199 chloride concentration, respectively.  $EC_{(inf)}$  and  $C_{Cl-(inf)}$  correspond to the electrical  
 200 conductivity and chloride concentration of the solution in the bio-cathodic compartment (i.e.,  
 201 the influent to the central compartment), respectively, to consider the chloride input due to  
 202 the acid dosage in this compartment.  $HRT'$  [d] is the hydraulic retention time of the central  
 203 compartment.

204 The coulombic efficiency for nitrate reduction ( $\varepsilon NO_x$ ) was calculated according to equation  
 205 6 (Viridis et al., 2008):

$$206 \quad \varepsilon NO_x [\%] = \frac{I}{n \Delta C_{NO_x} Q_{in} F} \times 100 \quad (6)$$

207 where  $I$  is the fixed current [A];  $n$  is the number of electrons that can be accepted by 1 mol  
 208 of oxidised nitrogen compound present in the bio-cathodic compartment, assuming  $N_2$  is the  
 209 final product;  $\Delta C_{NO_x}$  is the difference between the nitrate concentration in the cathodic  
 210 influent and effluent [ $mol NO_3^- - N L^{-1}$ ];  $Q_{in}$  is the influent flow rate [ $L s^{-1}$ ];  $F$  is Faraday's  
 211 constant [ $96485 C e^{-} mol^{-1}$ ].

212 The current efficiency (CE) was expressed as the percentage of the charge associated with  
 213 the chloride removed from the central compartment to the amount of electric charge  
 214 transferred (ECT) across the membranes (Ramírez-Moreno et al., 2019). CE [%] and ECT  
 215 [ $C m^{-3}$ ] were calculated using equations 7 and 8, respectively:

$$216 \quad CE [\%] = \frac{v z F (C_{Cl^- (inf)} - C_{Cl^- (eff)})}{ECT} \times 100 \quad (7)$$

$$217 \quad ECT [C m^{-3}] = \frac{\int I dt}{V} \quad (8)$$

218 where  $v$  and  $z$  represent the stoichiometric coefficient and the valence of the chloride ion,  
219 respectively;  $V$  [ $m^{-3}$ ] is the volume of water treated;  $dt$  is the time [s].

220 The specific energy consumption (SEC) was calculated according to equation 9 (Jingyu et  
221 al., 2017):

$$222 \quad SEC [kWh m^{-3}] = \frac{I \int E dt}{V} \quad (9)$$

223 where  $E$  is the cell potential [V].

## 224 **2.6 Analysis of bacterial communities by NGS of 16S rRNA gene**

225 The composition of the bacterial communities in the cathodic biofilm was characterised.

226 Samples of the biofilms formed on the bio-cathode were axenically collected at the end of

227 Test 5 (Table 1). Five cathode points were sampled, and the biomass was pooled into a

228 composite sample to mitigate the effects of microscale heterogeneity on the bio-cathode.

229 Biomass samples were stored at  $-20^{\circ}C$  before DNA extraction. Genomic DNA was extracted

230 from biomass samples (250 mg wet weight) using the DNeasy PowerSoil Pro Kit

231 (QIAGEN), and DNA was subsequently purified using the DNeasy PowerClean Cleanup Kit

232 (QIAGEN). The DNA quality and concentration were determined on agarose gel using a

233 DNA quantitation standard. DNA samples were submitted to Bio-Fab Research Srl (Rome,

234 Italy) for sequencing of the V3-V4 region of the bacterial 16S rRNA gene on an Illumina

235 Miseq platform (Illumina, San Diego, CA) using  $2 \times 300$  bp paired-end reads.

236 For data processing, raw sequences were demultiplexed by the sequencing facility. Reads

237 were trimmed to remove primer sequences using the CutAdapt version 3.5. Sequences were

238 imported into Quantitative Insights into Microbial Ecology (QIIME 2) version 2020-11

239 (Bolyen et al., 2019). Using the DADA2 pipeline (Callahan et al., 2016), reads with

240 ambiguous and poor-quality bases were discarded, good quality reads dereplicated and

241 denoised, and the paired reads merged. Chimeras and singletons were identified and

242 removed from the dataset. DADA2 was used to produce alternative sequence variants

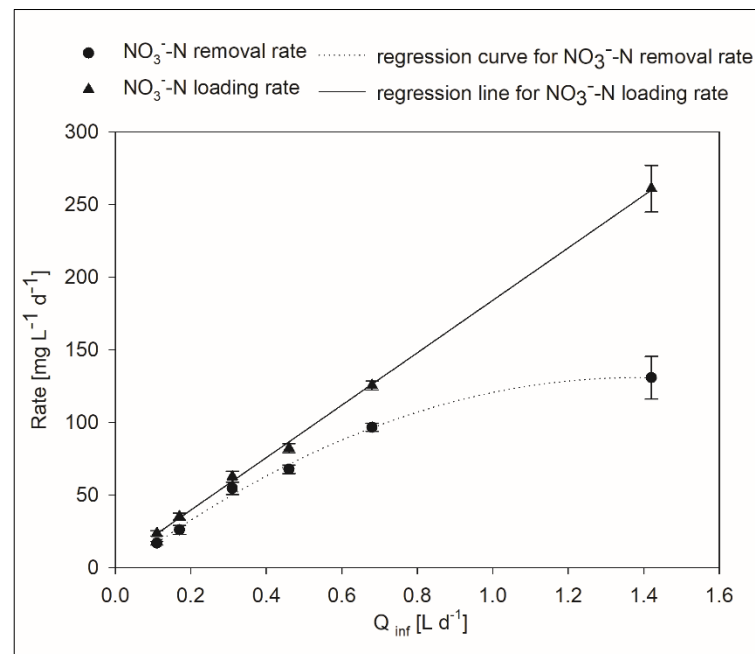


243 (ASVs), thus obtaining a filtered ASV-abundance table. For each ASV, a representative  
244 sequence was used for taxonomy assignment against the Silva database release 138 (Quast  
245 et al., 2013). The indices of diversity (richness as the number of observed ASV, Shannon  
246 with an e log base) and evenness (Pielou's) were used to assess the alpha-diversity by using  
247 the vegan R package (Oksanen et al., 2019). Read count data were normalised by Cumulative  
248 Sum Scaling (CSS) transformation using the metagenomeSeq package (Paulson et al., 2013).  
249 The Bray-Curtis similarity index between samples was calculated.

## 250 RESULTS AND DISCUSSION

### 251 3.1 Effect of the HRTs on denitrification and desalination performances

252 The system's enhancement was tested by increasing the influent flowrate and, thus, reducing  
253 the HRT within the system. Figure 1 shows the average  $\text{NO}_3^-$ -N loading and removal rates  
254 at different influent flowrates.



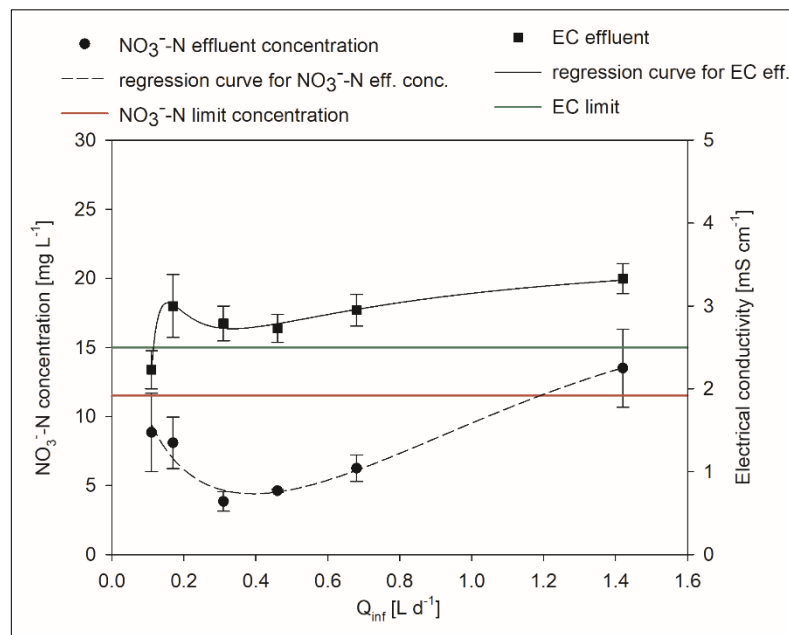
255  
256  
257 Figure 1. Average trend in nitrate-nitrogen loading into the system and nitrate-nitrogen removal rate as influent flowrate ( $Q_{inf}$ ) increases.

258 The nitrate loading rate was increased from  $23.6 \pm 1.8 \text{ mgNO}_3^- \text{-N L}^{-1} \text{d}^{-1}$  in Test 1 to  $261 \pm 16$   
259  $\text{mgNO}_3^- \text{-N L}^{-1} \text{d}^{-1}$  in Test 6 by reducing the HRT. Nitrogen removal rate increased (from

260  $16.9 \pm 1.3 \text{ mgNO}_3^- \text{-N L}^{-1} \text{d}^{-1}$  in Test 1 to  $130.8 \pm 14.7 \text{ mgNO}_3^- \text{-N L}^{-1} \text{d}^{-1}$  in Test 6) but did not  
 261 follow the same trend as the NLR, since a gradual deviation was observed.

262 The increase in the NRR with the influent flowrate could be explained by an increase in the  
 263 denitrification activity of the autotrophic biomass due to the proper supply of nitrate and  
 264 better hydrodynamic distribution (Pous et al., 2017; Vilà-Rovira et al., 2015).

265 Despite the increasing NRR, nitrate concentration in the effluent started to increase from  
 266 Test 4 onward (Figure 2). The nitrate effluent concentration remained below the legal limits  
 267 ( $< 11.3 \text{ mgNO}_3^- \text{-N L}^{-1}$  from the Nitrate Directive 91/767/EU) throughout the experiment  
 268 except during Test 6 (flowrate  $1.42 \text{ L d}^{-1}$  and HRT of  $2.4 \pm 0.2 \text{ h}$ ), which exceeded this limit  
 269 (with an average of  $13.5 \pm 2.8 \text{ mgNO}_3^- \text{-N L}^{-1}$ , corresponding to a N-RE of  $50 \pm 8 \%$ ).

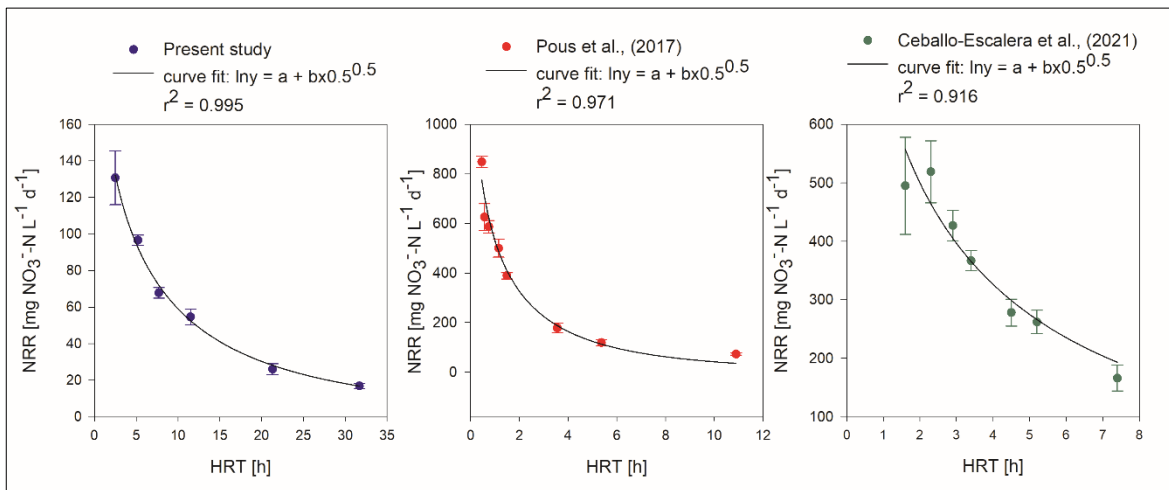


270  
 271  
 272

Figure 2. The average nitrate concentration and electrical conductivity (EC) trend in the effluent as influent flowrate increases.

273 During Test 6, low nitrite and nitrous oxide concentrations were detected in the effluent  
 274 ( $0.22 \pm 0.08 \text{ mgNO}_2^- \text{-N L}^{-1}$  and up to  $0.5 \text{ mgN}_2\text{O-N L}^{-1}$ , respectively). Therefore, it is evident  
 275 that during Test 6 (influent flowrate of  $1.42 \text{ L d}^{-1}$ ), limiting operating conditions were  
 276 reached for the system regarding nitrate removal.

277 Interestingly, the increase in nitrate removal rate as HRT decreased was also observed in  
 278 previous studies. Figure 3 compares the trend in nitrate removal rate versus the HRT for the  
 279 current study and those reported by Pous et al. (2017) and Ceballos-Escalera et al. (2021),  
 280 exploiting tubular systems with hydraulically connected anode and cathode compartments.  
 281 Although the systems were highly heterogeneous in terms of configuration (3-chamber plate  
 282 cell vs tubular cells), materials (graphite felt vs granular graphite), and operating conditions  
 283 (galvanostatic vs potentiostatic modes), the same mathematical model was able to fit the  
 284 observed NRR vs HRT relationship.



285 Figure 3. Comparison of nitrate removal rate (NRR) trends versus the HRT for the present study with that  
 286 reported by Pous et al. (2017) and Ceballos-Escalera et al. (2021) and modelling of results.  
 287

288 This result is interesting as it confirms that increasing the influent flowrate (and thus  
 289 reducing the HRT) can positively influence denitrification activity. Therefore, regardless of  
 290 the type of configuration or operating conditions used, the process behaviour with different  
 291 HRTs may be reasonably predicted, providing useful information in the perspective of  
 292 reactor scale-up.

293 A final test (Test 7) was carried out by bringing the HRT value back to that corresponding  
 294 to Test 5 (i.e.,  $4.9 \pm 0.4$  h) to restore the denitrifying process and verify microbial activity.  
 295 The performance in terms of nitrate removal observed during Test 5 ( $N\text{-RE} = 77 \pm 3\%$ , and  
 296  $N\text{-RR} = 96.7 \pm 2.8 \text{ mgNO}_3^- \text{-N L}^{-1} \text{d}^{-1}$ ) was immediately restored during Test 7, resulting in an

297 average N-RE of  $89\pm 4\%$  and N-RR of  $112\pm 7.5 \text{ mgNO}_3^- \text{-N L}^{-1} \text{d}^{-1}$ . In addition, while in Test  
298 6 (HRT of 1.4 h), the effluent concentration of nitrate exceeded the legal limits ( $13.5\pm 3$   
299  $\text{mgNO}_3^- \text{-N L}^{-1}$ ), the concentration was below the limits in Tests 5 and 7 ( $6\pm 1$  and  $3\pm 1$   
300  $\text{mgNO}_3^- \text{-N L}^{-1}$ , respectively). No nitrite or nitrous oxide were detected in the outlet during  
301 Test 7. The slight increase in performance observed between Test 5 and Test 7 demonstrates  
302 that biomass growth may have contributed in a small part to the increase in denitrifying  
303 performance. This result confirms the limiting conditions for denitrification reached in Test  
304 6, during which a general decline in terms of nitrate removal and production of intermediates  
305 were observed. However, this condition turned out to be reversible according to Test 7,  
306 demonstrating not a biomass inhibition condition but just an operational limit in Test 6. Since  
307 the applied current was initially much higher than that theoretically required to remove the  
308 nitrate input (10 mA applied vs approx. 1.4 mA theoretically required in Test 1), the  
309 coulombic efficiency for nitrate removal was always above 100%, decreasing as the HRT  
310 decreased, and reaching values close to 100% during Test 6.

311 An almost opposite trend to that of nitrate removal was observed for the desalination process.  
312 The desalination process showed the best performance in Test 1 (with an effluent  
313 conductivity of  $2.2\pm 0.2 \text{ mS cm}^{-1}$ ), which met the required limit of  $2.5 \text{ mS cm}^{-1}$  (98/83/CE  
314 Directive) but exceeded this value in Test 2 and gradually worsened in subsequent tests  
315 (Figure 2). Figure 4 shows the trend of electrical conductivity in the influent and effluent of  
316 the central desalination compartment and the desalination efficiency. As expected, the  
317 overall conductivity removal rate throughout the experiment was  $23.4\pm 7.3 \text{ mS cm}^{-1} \text{ d}^{-1}$ , so it  
318 did not vary substantially as the HRT decreased. Thus, the desalination trend was limited  
319 only by a physico-chemical effect due to insufficient charge replenishment as HRT  
320 decreases. This effect could easily be overcome by increasing the applied current in  
321 proportion to the increase in influent flowrate.

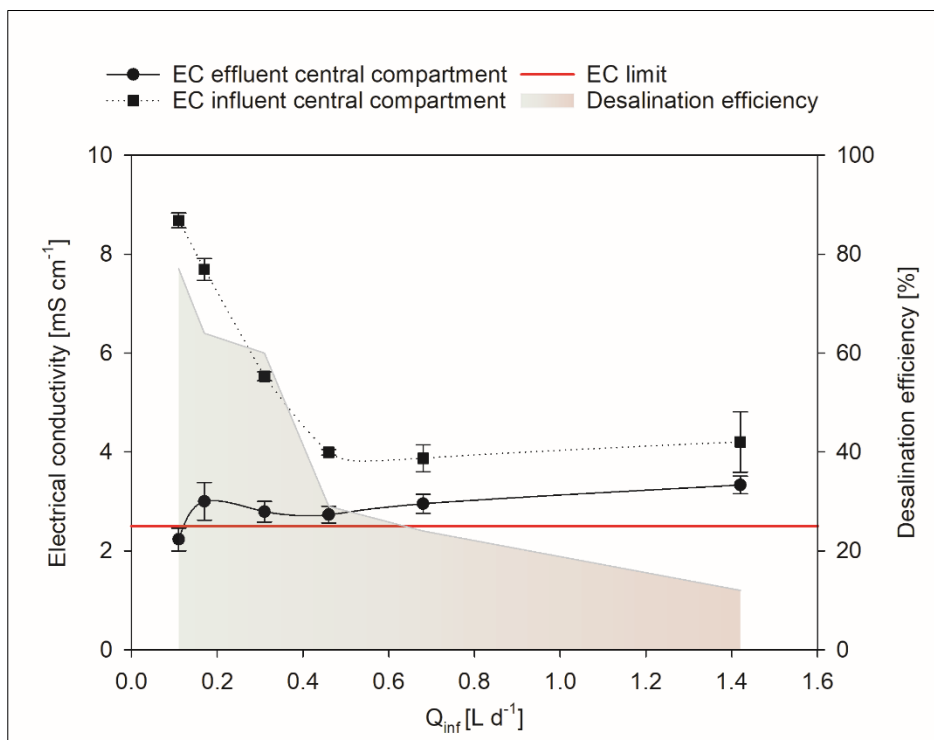


Figure 4. Average trend of central compartment influent and effluent electrical conductivity, and desalination efficiency versus the influent flowrate. The red line indicates the electrical conductivity limit for freshwater (2.5 mS cm<sup>-1</sup>).

322  
323  
324  
325

326 The influent conductivity of the central desalination compartment (corresponding to the  
327 effluent of the bio-cathode compartment) dropped from 8.7±0.2 mS cm<sup>-1</sup> in Test 1 to 4.2±0.6  
328 mS cm<sup>-1</sup> in Test 6, likely as a result of the increased influent flowrate which probably led to  
329 a faster turnover of the solution in the bio-cathodic compartment, reducing the accumulation  
330 of both Cl<sup>-</sup> ions due to the acid dosage, and cations migrating from the central compartment  
331 through the CEM. The average chloride concentration measured in the cathode chamber (and  
332 thus including the influent and acid dosage) decreased from 3622±443 in Test 1 to 1385±56  
333 mgCl<sup>-</sup> L<sup>-1</sup> in Test 6, while the sodium concentration decreased from 2355±370 to 1040±182  
334 mgNa<sup>+</sup> L<sup>-1</sup>, respectively, for Test 1 and Test 6.

335 On the other hand, the effluent electrical conductivity increased slightly to 3.3 mS cm<sup>-1</sup>. The  
336 electrical conductivity trend in the bio-cathode compartment and effluent trend resulted in a  
337 reduction of the overall desalination efficiency, which dropped to 12±2% in the last test  
338 (from 77±13% in Test 1). Coherently, the current efficiency related to the removal of  
339 chloride in the central compartment decreased during the experiment from 89±14% in Test

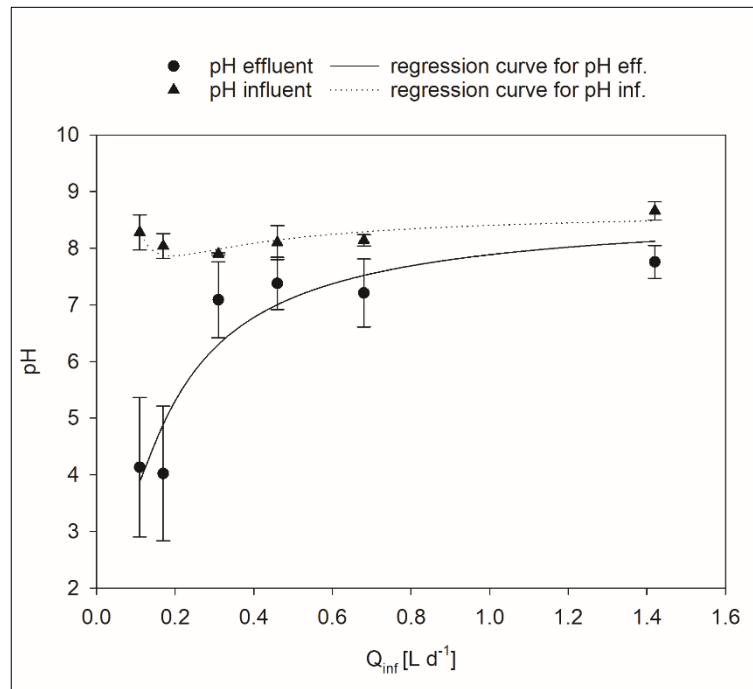
340 1 to  $59\pm 15\%$  in Test 6. This performance could be related to the variation of the influent  
341 flowrate and may be explained by insufficient HRT (passing from  $6.7\pm 0.3$  h in Test 1 to  
342  $0.5\pm 0.02$  h in Test 6) in the central desalination compartment. Calculating the theoretical  
343 quantity of chloride ions that can be transferred through the membranes by applying a current  
344 of 10 mA to the varying HRT gives  $2.8$  g L<sup>-1</sup> for Test 1 and  $0.22$  g L<sup>-1</sup> for Test 6. These  
345 values are very close to those actually obtained and correspond to  $2.5\pm 0.4$  and  $0.13\pm 0.03$   
346 gCl<sub>removed</sub> L<sup>-1</sup>, respectively, for Test 1 and Test 6, confirming the above results. Thus, the  
347 HRT decrease did not allow sufficient ions to migrate through the membranes to observe a  
348 significant reduction in effluent electrical conductivity. The adverse effect of low HRT on  
349 desalination performance was already demonstrated for the technology closest to the present  
350 study, i.e., MDCs (microbial desalination cells). Indeed, Jingyu et al. (2017) reported that  
351 HRT influences the removal of total dissolved solutes (TDS), increasing with the HRT,  
352 resulting in a higher current generation in MDC.

353 Chlorine production in the anodic compartment was monitored throughout the whole  
354 experimentation, and an average chlorine concentration of  $14\pm 3$  mgCl<sub>2</sub> L<sup>-1</sup> was observed.  
355 An essential aspect of monitoring is the durability of materials in contact with chlorine, as it  
356 is a powerful oxidant, and it tends to attack and damage them. For this reason, it was decided  
357 to replace the solution in the anodic chamber periodically (about every 10 days, producing  
358 an average concentration of  $16\pm 1$  mgCl<sub>2</sub> L<sup>-1</sup>) to avoid system damage. Higher values of  
359 chlorine concentration (approx.  $30$  mgCl<sub>2</sub> L<sup>-1</sup>) were obtained by Puggioni et al. (2021) in the  
360 same system at the highest HRT tested but without the periodic replacement of the solution.  
361 In addition to being an effective disinfectant, chlorine has the additional advantage that its  
362 residue can protect the downstream flow from the point of disinfection (the WHO  
363 recommends a residual concentration of free chlorine greater than or equal to  $0.5$  mg L<sup>-1</sup>  
364 after at least 30 minutes of contact with a pH below 8.0).

365 **3.2 Considerations on pH development during the process**

366 Increasing the influent flow rate also had an effect on pH trend in the different compartments.  
367 pH control plays a significant role in ensuring optimal denitrifying microbial activity, as a  
368 neutral pH is strictly necessary for this biological process (Clauwaert et al., 2009). Such  
369 control has become essential to optimise water desalination performance. Several studies  
370 demonstrated that the pH gradient between the anode and cathode compartments could lead  
371 to potential losses (of approximately 0.095 V) that adversely affect the desalination  
372 efficiencies of MDCs (Jingyu et al., 2017).

373 During the experiment, the periodic dosage of acid to control the pH in the bio-cathodic  
374 compartment remained constant over the entire experimental period. This occurrence  
375 resulted in a difference mainly in the effluent pH as a function of the influent flowrate. Figure  
376 5 shows that while the influent pH mainly remained constant, the effluent pH increased from  
377 near-acidic ( $4.1 \pm 1.2$ ) in Test 1 to slightly alkaline ( $7.8 \pm 0.3$ ) in Test 6.  
378



379

380 Figure 5. Average influent and effluent pH trend versus the influent  
381 flowrate.

382 Acidic pH values in the effluent corresponding to the first tests may be due to the higher  
383 HRT in the central desalination chamber ( $6.7\pm 0.3$  h in Test 1) that allowed protons produced  
384 at the anode ( $\text{pH } 2.0\pm 0.7$ ) to pass through the AEM, because of their small size. By reducing  
385 the HRT (to  $0.5\pm 0.02$  h in Test 6) as the influent flowrate increased, the solution replacement  
386 led to a slowing down of the pH increase in the bio-cathode compartment and a lower  
387 passage of protons through the AEM into the effluent. In addition, the acid dosage per  $\text{m}^3$  of  
388 treated water was reduced as the influent flowrate increased, which means lower operating  
389 costs for pH balancing.

### 390 **3.3 Bacterial community diversity on the bio-cathode of the 3-compartment BES**

391 Cathodic biomass was collected at the end of Test 5. The bacterial community composition  
392 of the biomass is shown in Figure 7A. The most abundant phyla of Bacteria in the biomass  
393 were Proteobacteria (44.0%) followed by Actinobacteriota (16.0%), Firmicutes (11.8%),  
394 Bacteroidota (10.8%), Planctomycetota (5.1%) and Chloroflexi (4.8%). The other less  
395 abundant phyla were all below the 3%, while the unassigned sequences accounted for 1.1%  
396 in the composition of bacterial community. At order level, the most abundant taxa were  
397 Rhizobiales (17.0%), Corynebacteriales (7.4%), and Burkholderiales (6.6%), followed by  
398 Xanthomonadales (4.5%), Alteromonadales (4.3%), and Thermomicrobiales (4.2%). At  
399 genus level, seven most abundant taxa accounted for more than 20% of the total community,  
400 including the genera *Rhizobium* (3.9%) and *Bosea* (3.1%) in Rhizobiales, *Mycobacterium*  
401 (3.2%) and *Gordonia* (2.4%) in Corynebacteriales, *Fontibacter* (2.6%) in Cytophagales,  
402 *Clostridium sensu strictu* (2.4%) in Firmicutes as well as the uncultured JG30-KF-CM45 in  
403 Thermomicrobiales (3.2%).

404 In order to compare the biomass established under the galvanostatic mode (GM), used in the  
405 present study, and potentiostatic mode, previously tested by Puggioni et al. (2021), a sample  
406 of the biofilm formed on the bio-cathode of the cell working in potentiostatic mode (PM)

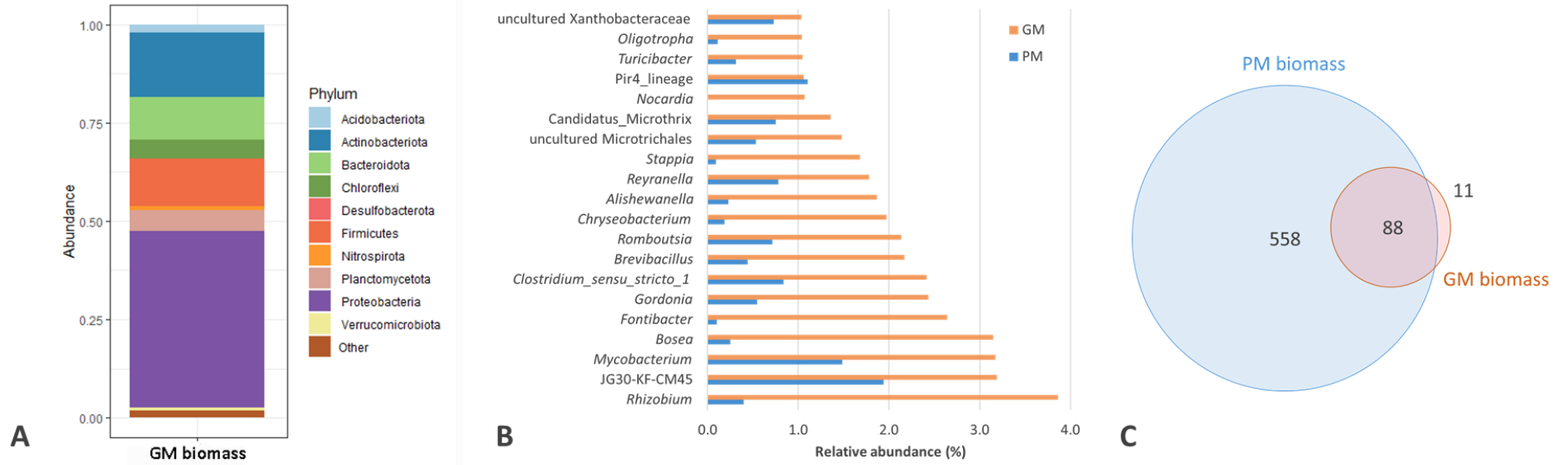


407 was also analysed and the difference in the bacterial communities between the GM and PM  
408 biomass investigated in terms of alpha-diversity and community composition.

409 The community in GM biomass was characterised by a minor bacterial alpha-diversity as  
410 highlighted by a lower number of ASVs (i.e., reduced richness) and a higher community  
411 dominance (i.e., reduced evenness) in comparison to the PM biomass (Table S1). A marked  
412 difference in the bacterial community composition was also evident at the different  
413 taxonomic ranks. As compared to the PM biomass, the GM bio-cathodic community is  
414 characterised by the increase in the relative abundances (RAs) of Proteobacteria (+11.2%)  
415 and Firmicutes (+6.4%), and the decrease in RAs of Planctomycetota (-8.9%) and  
416 Chloroflexi (-7.3%). At order level, the more pronounced changes in RAs were the  
417 enrichment in Rhizobiales (+7.9%), Corynebacteriales (+5.3%), Alteromonadales (+3.5%),  
418 and Xanthomonadales (+3.4%). The comparison between PM and GM also showed the  
419 reduction in Pirellulales (-3.1%). Moreover, Caldilineales and Anaerolineales were not  
420 detected in the GM cathodic biofilm, while they accounted for 3.4% and 2.6% in the PM  
421 biomass, respectively. At genus level, the highest differences were found for the taxa  
422 *Rhizobium*, *Bosea*, *Fontibacter*, *Gordonia*, which were all below the 0.5% in PM biomass,  
423 while they predominated the composition of GM bacterial community (Figure 7B). Out of  
424 the 646 ASVs found in the PM biomass, 88 ASVs were shared between the two  
425 communities, while 11 and 558 ASVs were unique of GM and PM biomass, respectively  
426 (Figure 7C). Among the ASVs unique of the GM biomass, ASV01 affiliated to an uncultured  
427 lineage of Burkholderiales was also the most abundant ASV, accounting for 2.5% of the GM  
428 bacterial community (Table S2). Other ASVs exclusively found in the GM biomass were  
429 ASV026 (1.1%) and ASV027 (1.1%) affiliated to the genera *Fontibacter* and *Nocardia*,  
430 respectively.

431 Overall, biodiversity was severely restricted under galvanostatic mode. Presented results  
432 suggested that test conditions exerted a selective pressure on the bacterial community of the  
433 cathodic biofilm influencing its organisation and enriching few dominant populations.  
434 Moreover, an active role in denitrifying biomass has been previously proposed for several  
435 bacteria dominating the GM bio-cathodic biomass. More specifically, isolates affiliated to  
436 Rhizobiales have been proved to denitrify under autotrophic and heterotrophic conditions  
437 (Vilar-Sanz et al., 2108), and the genus *Rhizobium* has been implied in denitrification in  
438 MFC system for treating saline wastewater (Xu et al., 2019). *Clostridium sensu strictu* has  
439 been detected at a high amount in MEC biomass and suggested to be responsible for  
440 autotrophic denitrification in a bioelectrochemically-assisted constructed wetland system  
441 (Sotres et al., 2015; Xu et al., 2017). Recently, the genus *Fontibacter* has been found to be  
442 enriched after long term adaptation in a BES for nitrate removal from coke wastewater  
443 effluent (Tang et al., 2017) and a species of the genus, isolated from an MFC, has been  
444 proved to couple oxidation of organic matter to Fe(III) reduction (Zhang et al., 2013). On  
445 the contrary, other dominant populations in the GM biomass, such as Corynebacteriales,  
446 have been less extensively described, and their metabolic role in bioelectrochemical systems  
447 is far to be undiscovered.

448 **Figure 7.** Bacterial communities of the biofilms formed on the bio-cathode of the 3-compartment bio-electrochemical cells **A:** Bar plot showing the contribution at phylum level  
 449 in cathodic biomass under galvanostatic mode (GM). **B:** twenty most abundant genera in GM biomass and comparison with biomass established under potentiostatic mode (PM).  
 450 **C:** Venn chart showing the overlap of ASVs in bacterial communities of cathodic GM and PM biomasses.



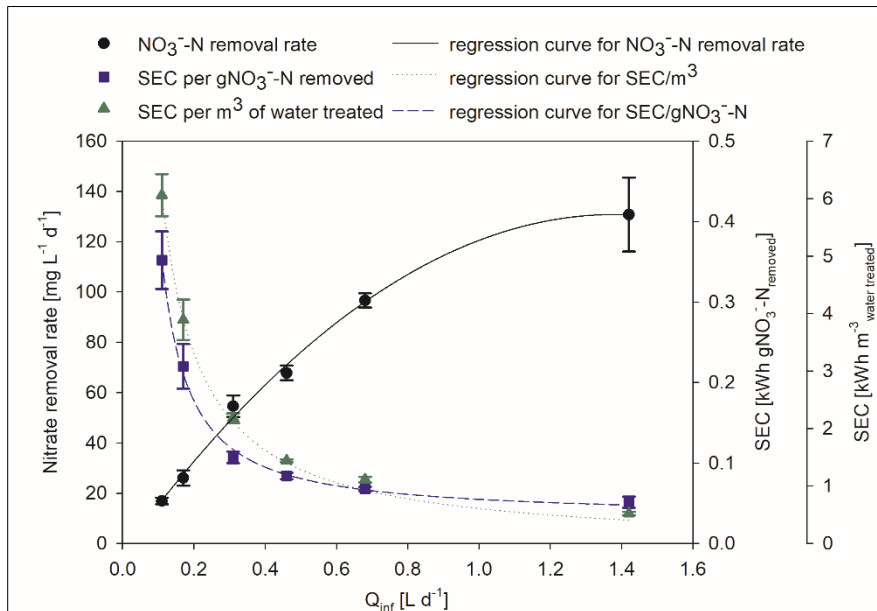
451  
 452  
 453

454 **3.4 Sustainability perspective on the application of BES for simultaneous**  
 455 **denitrification and desalination**

456 In order to move towards scaling-up of the technology for groundwater treatment, the system  
 457 must be both technically and economically feasible. For this reason, a preliminary cost-  
 458 benefit analysis was carried out comparing the main operational costs associated with the  
 459 technology and the potential benefits obtained according to experimental data.

460 The operating costs of a technology depend significantly on the energy consumption of the  
 461 process. Figure 6 presents the profiles of the specific energy consumption (SEC) per gram  
 462 of  $\text{NO}_3^-$ -N removed and SEC per volume of water treated as a function of influent flowrate  
 463 and compared with the trend in nitrate removal rate.

464 During the experiment, an optimisation was observed not only in the removal of nitrate but  
 465 also in energy consumption, which was significantly reduced to values of  $5.1 \cdot 10^{-2} \pm 0.7 \cdot 10^{-2}$   
 466  $\text{kWh g}^{-1}\text{NO}_3^-$ -N<sub>removed</sub> and  $0.5 \pm 0.03 \text{ kWh m}^{-3}$  water treated (starting from  $35.2 \cdot 10^{-2} \pm 3.6 \cdot 10^{-2} \text{ kWh}$   
 467  $\text{g}^{-1}\text{NO}_3^-$ -N<sub>removed</sub> and  $6.1 \pm 0.4 \text{ kWh m}^{-3}$  water treated, respectively).



468 Figure 6. Average trends in specific energy consumed (SEC) per gram of nitrate-  
 469 nitro-nitrogen removed and per volume of water treated, and nitrate removal rate as the  
 470 inlet flow rate changes.  
 471

472 Pous et al. (2015) reported a list of specific energy consumptions for various technologies  
473 such as bioelectrochemical systems (BES), biofilm electrode reactor (BER), membrane  
474 bioreactor (MBR), electrodialysis (ED) and reverse osmosis (RO) (Zhao et al., 2011;  
475 Twomey et al., 2010; McAdam and Judd, 2008; Ortiz et al., 2008). Compared to the reported  
476 values, the energy consumption per  $\text{m}^3$  of treated water was within the consumption range  
477 reported for desalination technologies, i.e., electrodialysis and reverse osmosis (between  
478 0.04 and 2.09  $\text{kWh m}^{-3}$  treated water). The energy consumption per gram of nitrate removed  
479 obtained in the present study was in line with those of the technologies reported for nitrate  
480 removal only (BES and BER mainly), thus between  $0.16 \cdot 10^{-2}$  and  $7 \cdot 10^{-2}$   $\text{kWh g}^{-1}\text{NO}_3^-$ -  
481  $\text{N}_{\text{removed}}$ . Specifically, the values obtained in this study are closer to those of BER ( $7 \cdot 10^{-2}$   
482  $\text{kWh g}^{-1}\text{NO}_3^- \cdot \text{N}_{\text{removed}}$ ), which applies a potential difference between the electrodes, in  
483 contrast to BES where the potential of the cathode electrode is fixed. This type of catalytical  
484 operation produces hydrogen in the cathode chamber, which is then used by bacteria to  
485 reduce nitrate. In the present study, the current was fixed, and the potential established at the  
486 cathode (approximately -1.3 V vs Ag/AgCl) was suitable for hydrogen production.  
487 According to Pous et al. (2015), fixing the cathode potential makes it possible to control the  
488 reduction of nitrate in the end products and implies less energy consumption. In the present  
489 study, however, the aim is not only to remove nitrate but also to reduce the electrical  
490 conductivity of water, as well as the production of value-added products (chlorine). In fact,  
491 during the process, part of the chloride accumulated in the solution of the anodic  
492 compartment is converted into free chlorine (Puggioni et al., 2021). Thus, the energy applied  
493 is used to carry out three processes simultaneously with consumption comparable to systems  
494 carrying out a single process (i.e., only denitrification or desalination). Under optimal  
495 operating conditions (HRT =  $4.9 \pm 0.4$  h), the total cost of energy consumption is  $0.23 \text{ € m}^{-3}$ ,  
496 assuming an energy cost of  $0.21 \text{ € kWh}^{-1}$  (Eurostat, 2021). This value is competitive,

497 considering that Ceballos-Escalera et al. (2022) estimated an operating cost of 0.14 € m<sup>-3</sup>  
498 only for the bio-electrochemical nitrate removal.

499 From an economic point of view, the production of chlorine also plays an important role.  
500 Chlorine is a disinfectant agent that is highly used in water treatment plants, and its market  
501 value is growing significantly due to the rising demand from the agrochemical and  
502 pharmaceutical industries. Moreover, the rising demand for water treatment applications  
503 combined with increased awareness of better hygiene practices resulting from the impact of  
504 the Sars-CoV-2 pandemic will drive the need for chlorine among industrialists. Greaves et  
505 al. (2022) demonstrated that Sars-CoV-2 is successfully eliminated by disinfection with free  
506 chlorine in both deionised water and wastewater. Web-based chlorine market data show a  
507 forecast growth of the chlorine value at a CAGR (compound annual growth rate) between  
508 3.5 and 4.5% for the period 2021-2027.

509 In the present study, up to 0.17 gCl<sub>2</sub> per gCl<sub>removed</sub> was produced, and this production can  
510 easily be increased by switching to a continuous mode in the anodic chamber or by stripping  
511 the chlorine produced. In fact, Puggioni et al. (2021) showed higher production rates at the  
512 start of the batch that gradually decreased to a plateau over long periods of operation.  
513 Therefore, switching to continuous mode would increase production rates while avoiding  
514 chlorine accumulation and excessive concentrations in the anode chamber. Optimising the  
515 chlorine capture system seems essential to maximise its production and reduce the contact  
516 time with the materials in the bioelectrochemical cell.

517

518

#### 519 4. CONCLUSIONS

520 At higher flowrates (and lower HRT, between  $7.3\pm 0.6$  and  $2.4\pm 0.2$  h), an increase in  
521 nitrate removal was found, reaching removal rates of  $131 \text{ mgNO}_3^- \cdot \text{N L}^{-1} \cdot \text{d}^{-1}$ . The operating  
522 limit for denitrification was reached at an HRT of  $2.4\pm 0.2$  h, during which an effluent  
523 nitrate concentration above legal limits (91/767/EU) and the presence of intermediates  
524 were observed. Desalination performance was reduced (from  $77\pm 13\%$  in Test 1 to  $12\pm 2\%$   
525 in Test 6), but the effluent electrical conductivity remained close to the legal limits  
526 (98/83/CE). In addition, biodiversity in the cathodic biomass was severely restricted  
527 under galvanostatic mode and populations previously identified under denitrifying  
528 conditions in BES were enriched.

529 The tests carried out in the present study demonstrate the economic potential of the  
530 proposed technology thanks to the possibility of considerably reducing energy  
531 consumption while simultaneously increasing denitrification performance. Such result  
532 was achieved simply by acting on the treated flowrate (by reducing hydraulic retention  
533 times) and not on the reactor volumes, which would imply additional costs in terms of  
534 materials and space. Finally, chlorine production represents an enormous potential for  
535 possible real application as it would reduce the costs of any on-site disinfection or, in  
536 general, an economic return if it were to be resold.

#### 537 ACKNOWLEDGEMENTS

538 This work was funded through the Fondo di Sviluppo e Coesione 2014-2020, Patto per  
539 lo sviluppo della Regione Sardegna - Area Tematica 3 - Linea d' Azione 3.1, "Interventi  
540 di sostegno alla ricerca". Project SARdNAF "Advanced Systems for the Removal of  
541 Nitrates from Groundwater", ID: RASSR53158. S.P. is a Serra Hunter Fellow (UdG-AG-  
542 575) and acknowledges the funding from the ICREA Academia award. LEQUIA has been

543 recognised as a consolidated research group by the Catalan Government (2017-SGR-  
544 1552). The authors would like to thank Ms. Orietta Masala (CNR-IGAG) for her support  
545 with the ICP/OES analysis.

## 546 REFERENCES

- 547 Beretta, G., Daghighi, M., Espinoza Tofalos, A., Franzetti, A., Mastorgio, A.F., Saponaro,  
548 S., Sezenna, E., 2020. Microbial Assisted Hexavalent Chromium Removal in  
549 Bioelectrochemical Systems. *Water* 12, 466. <https://doi.org/10.3390/w12020466>
- 550 Bolyen, E., Rideout, J. R., Dillon, M. R., Bokulich, N. A., Abnet, C. C., Al-Ghalith, G.  
551 A., et al.. (2019). Reproducible, interactive, scalable and extensible microbiome  
552 data science using QIIME 2. *Nature Biotechnology*, 37(8), 852–857.  
553 <https://doi.org/10.1038/s41587-019-0209-9>
- 554 Callahan, B. J., McMurdie, P. J., Rosen, M. J., Han, A. W., Johnson, A. J. A., & Holmes,  
555 S. P. (2016). DADA2: High-resolution sample inference from Illumina amplicon  
556 data. *Nature Methods*, 13(7), 581–583. <https://doi.org/10.1038/nmeth.3869>
- 557 Ceballos-Escalera, A., Pous, N., Balaguer, M.D., Puig, S., 2022. Electrochemical water  
558 softening as pretreatment for nitrate electro bioremediation. *Sci. Total Environ.*  
559 806, 150433. <https://doi.org/10.1016/j.scitotenv.2021.150433>
- 560 Ceballos-Escalera, A., Pous, N., Chiluiza-Ramos, P., Korth, B., Harnisch, F., Bañeras, L.,  
561 Balaguer, M.D., Puig, S., 2021. Electro-bioremediation of nitrate and arsenite  
562 polluted groundwater. *Water Res.* 190, 116748.  
563 <https://doi.org/10.1016/j.watres.2020.116748>
- 564 Clauwaert, P., Desloover, J., Shea, C., Nerenberg, R., Boon, N., Verstraete, W., 2009.  
565 Enhanced nitrogen removal in bio-electrochemical systems by pH control.  
566 *Biotechnol. Lett.* 31, 1537–1543. <https://doi.org/10.1007/s10529-009-0048-8>



567 Electricity price statistics [WWW Document], n.d. URL  
568 [https://ec.europa.eu/eurostat/statistics-](https://ec.europa.eu/eurostat/statistics-explained/index.php?title=Electricity_price_statistics)  
569 [explained/index.php?title=Electricity\\_price\\_statistics](https://ec.europa.eu/eurostat/statistics-explained/index.php?title=Electricity_price_statistics) (accessed 11.29.21).

570 Greaves, J., Fischer, R.J., Shaffer, M., Bivins, A., Holbrook, M.G., Munster, V.J., Bibby,  
571 K., 2022. Sodium hypochlorite disinfection of SARS-CoV-2 spiked in water and  
572 municipal wastewater. *Sci. Total Environ.* 807, 150766.  
573 <https://doi.org/10.1016/j.scitotenv.2021.150766>

574 Janža, M., 2022. Optimisation of well field management to mitigate groundwater  
575 contamination using a simulation model and evolutionary algorithm. *Sci. Total*  
576 *Environ.* 807, 150811. <https://doi.org/10.1016/j.scitotenv.2021.150811>

577 Jingyu, H., Ewusi-Mensah, D., Norgbey, E., 2017. Microbial desalination cells  
578 technology: a review of the factors affecting the process, performance and  
579 efficiency. *Desalination and Water Treatment.* 87, 140–159.  
580 <https://doi.org/10.5004/dwt.2017.21302>

581 Kwon, E., Park, J., Park, W.-B., Kang, B.-R., Woo, N.C., 2021. Nitrate contamination of  
582 coastal groundwater: Sources and transport mechanisms along a volcanic aquifer.  
583 *Sci. Total Environ.* 768, 145204. <https://doi.org/10.1016/j.scitotenv.2021.145204>

584 Lian, J., Tian, X., Guo, J., Guo, Y., Song, Y., Yue, L., Wang, Y., Liang, X., 2016. Effects  
585 of resazurin on perchlorate reduction and bioelectricity generation in microbial  
586 fuel cells and its catalysing mechanism. *Biochem. Eng. J.* 114, 164–172.  
587 <https://doi.org/10.1016/j.bej.2016.06.028>

588 McAdam, E.J., Judd, S.J., 2008. Immersed membrane bioreactors for nitrate removal  
589 from drinking water: Cost and feasibility. *Desalination* 231, 52–60.  
590 <https://doi.org/10.1016/j.desal.2007.11.038>

591 Oksanen, J., Blanchet, F. G., Friendly, M., Kindt, R., Legendre, P.,McGlinn, D., et al.  
592 (2019). Vegan. Community Ecology Package.

593 Ortiz, J., Exposito, E., Gallud, F., Garcíagarcía, V., Montiel, V., Aldaz, A., 2008.  
594 Desalination of underground brackish waters using an electro dialysis system  
595 powered directly by photovoltaic energy. Sol. Energy Mater. Sol. Cells 92, 1677–  
596 1688. <https://doi.org/10.1016/j.solmat.2008.07.020>

597 Palma, E., Daghighi, M., Franzetti, A., Petrangeli Papini, M., Aulenta, F., 2018. The  
598 bioelectric well: a novel approach for *in situ* treatment of hydrocarbon-  
599 contaminated groundwater. Microb. Biotechnol. 11, 112–118.  
600 <https://doi.org/10.1111/1751-7915.12760>

601 Patil, S., Harnisch, F., Schröder, U., 2010. Toxicity Response of Electroactive Microbial  
602 Biofilms-A Decisive Feature for Potential Biosensor and Power Source  
603 Applications. ChemPhysChem 11, 2834–2837.  
604 <https://doi.org/10.1002/cphc.201000218>

605 Paulson, J. N., Colin Stine, O., Bravo, H. C., & Pop, M. (2013). Differential abundance  
606 analysis for microbial marker-gene surveys. Nature Methods, 10(12), 1200–1202.  
607 <https://doi.org/10.1038/nmeth.2658>

608 Pous, N., Balaguer, M.D., Colprim, J., Puig, S., 2018. Opportunities for groundwater  
609 microbial electro-remediation. Microb. Biotechnol. 11, 119–135.  
610 <https://doi.org/10.1111/1751-7915.12866>

611 Pous, N., Puig, S., Balaguer, M.D., Colprim, J., 2017. Effect of hydraulic retention time  
612 and substrate availability in denitrifying bioelectrochemical systems. Environ.  
613 Sci. Water Res. Technol. 3, 922–929. <https://doi.org/10.1039/C7EW00145B>

614 Pous, N., Puig, S., Dolores Balaguer, M., Colprim, J., 2015. Cathode potential and anode  
615 electron donor evaluation for a suitable treatment of nitrate-contaminated

616 groundwater in bioelectrochemical systems. *Chem. Eng. J.* 263, 151–159.  
617 <https://doi.org/10.1016/j.cej.2014.11.002>

618 Puggioni, G., Milia, S., Dessì, E., Unali, V., Pous, N., Balaguer, M.D., Puig, S., Carucci,  
619 A., 2021. Combining electro-bioremediation of nitrate in saline groundwater with  
620 concomitant chlorine production. *Water Res.* 206, 117736.  
621 <https://doi.org/10.1016/j.watres.2021.117736>

622 Quast, C., Pruesse, E., Yilmaz, P., Gerken, J., Schweer, T., Yarza, P., et al. (2013). The  
623 SILVA ribosomal RNA gene database project: improved data processing and  
624 web-based tools. *Nucleic Acids Res.* 41, 590–596. doi: 10.1093/nar/gks1219

625 Ramírez-Moreno, M., Rodenas, P., Aliaguilla, M., Bosch-Jimenez, P., Borràs, E.,  
626 Zamora, P., Monsalvo, V., Rogalla, F., Ortiz, J.M., Esteve-Núñez, A., 2019.  
627 Comparative Performance of Microbial Desalination Cells Using Air Diffusion  
628 and Liquid Cathode Reactions: Study of the Salt Removal and Desalination  
629 Efficiency. *Front. Energy Res.* 7, 135. <https://doi.org/10.3389/fenrg.2019.00135>

630 Serio, F., Miglietta, P.P., Lamastra, L., Ficocelli, S., Intini, F., De Leo, F., De Donno, A.,  
631 2018. Groundwater nitrate contamination and agricultural land use: A grey water  
632 footprint perspective in Southern Apulia Region (Italy). *Sci. Total Environ.* 645,  
633 1425–1431. <https://doi.org/10.1016/j.scitotenv.2018.07.241>

634 Sevda, S., Sreekishnan, T.R., Pous, N., Puig, S., Pant, D., 2018. Bioelectroremediation of  
635 perchlorate and nitrate contaminated water: A review. *Bioresour. Technol.* 255,  
636 331–339. <https://doi.org/10.1016/j.biortech.2018.02.005>

637 Sotres, A., Cerrillo, M., Viñas, M., & Bonmatí, A. (2015). Nitrogen recovery from pig  
638 slurry in a two-chambered bioelectrochemical system. *Bioresource Technology*,  
639 194, 373–382. <https://doi.org/10.1016/j.biortech.2015.07.036>

640 Tang, R., Wu, D., Chen, W., Feng, C., & Wei, C. (2017). Biocathode denitrification of  
641 coke wastewater effluent from an industrial aeration tank: Effect of long-term  
642 adaptation. *Biochemical Engineering Journal*, 125, 151–160.  
643 <https://doi.org/10.1016/j.bej.2017.05.022>

644 Twomey, K.M., Stillwell, A.S., Webber, M.E., 2010. The unintended energy impacts of  
645 increased nitrate contamination from biofuels production. *J Env. Monit* 12, 218–  
646 224. <https://doi.org/10.1039/B913137J>

647 Verdini, R., Aulenta, F., de Tora, F., Lai, A., Majone, M., 2015. Relative contribution of  
648 set cathode potential and external mass transport on TCE dechlorination in a  
649 continuous-flow bioelectrochemical reactor. *Chemosphere* 136, 72–78.  
650 <https://doi.org/10.1016/j.chemosphere.2015.03.092>

651 Vilà-Rovira, A., Puig, S., Balaguer, M.D., Colprim, J., 2015. Anode hydrodynamics in  
652 Bioelectrochemical Systems 9. RSC Advances.  
653 <https://pubs.rsc.org/en/Content/ArticleLanding/2015/RA/c5ra11995b>

654 Vilar-Sanz, A., Pous, N., Puig, S., Balaguer, M. D., Colprim, J., & Bañeras, L. (2018).  
655 Denitrifying nirK-containing alphaproteobacteria exhibit different electrode  
656 driven nitrite reduction capacities. *Bioelectrochemistry*, 121, 74–83.  
657 <https://doi.org/10.1016/j.bioelechem.2018.01.007>

658 Viridis, B., Rabaey, K., Yuan, Z., Keller, J., 2008. Microbial fuel cells for simultaneous  
659 carbon and nitrogen removal. *Water Res.* 42, 3013–3024.  
660 <https://doi.org/10.1016/j.watres.2008.03.017>

661 Wang, C., Dong, J., Hu, W., Li, Y., 2021. Enhanced simultaneous removal of nitrate and  
662 perchlorate from groundwater by bioelectrochemical systems (BESs) with

663 cathodic potential regulation. *Biochem. Eng. J.* 173, 108068.  
664 <https://doi.org/10.1016/j.bej.2021.108068>

665 Wang, X., Aulenta, F., Puig, S., Esteve-Núñez, A., He, Y., Mu, Y., Rabaey, K., 2020.  
666 Microbial electrochemistry for bioremediation. *Environ. Sci. Ecotechnology* 1,  
667 100013. <https://doi.org/10.1016/j.esec.2020.100013>

668 Xu, D., Xiao, E., Xu, P., Zhou, Y., He, F., Zhou, Q., ... Wu, Z. (2017). Performance and  
669 microbial communities of completely autotrophic denitrification in a  
670 bioelectrochemically-assisted constructed wetland system for nitrate removal.  
671 *Bioresource Technology*, 228, 39–46.  
672 <https://doi.org/10.1016/j.biortech.2016.12.065>

673 Xu, F., Ouyang, D. long, Rene, E. R., Ng, H. Y., Guo, L. ling, Zhu, Y. jie, Kong, Q.  
674 (2019). Electricity production enhancement in a constructed wetland-microbial  
675 fuel cell system for treating saline wastewater. *Bioresource Technology*,  
676 288(May), 121462. <https://doi.org/10.1016/j.biortech.2019.121462>

677 Zhang, Y., Angelidaki, I., 2013. A new method for in situ nitrate removal from  
678 groundwater using submerged microbial desalination–denitrification cell  
679 (SMDDC). *Water Res.* 47, 1827–1836.  
680 <https://doi.org/10.1016/j.watres.2013.01.005>

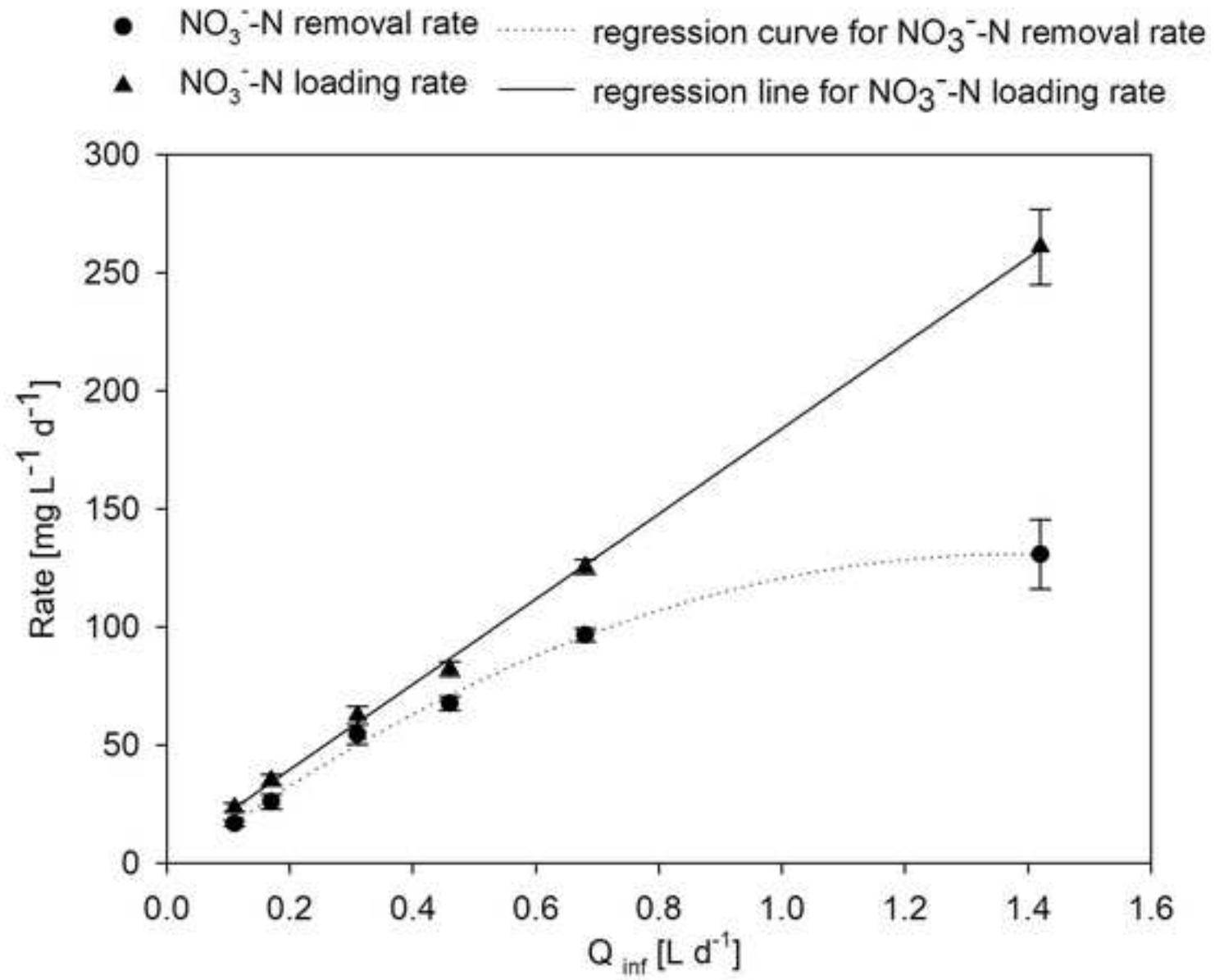
681 Zhang, J., Yang, G. Q., Zhou, S., Wang, Y., Yuan, Y., & Zhuang, L. (2013). *Fontibacter*  
682 *ferrireducens* sp. nov., an Fe(III)-reducing bacterium isolated from a microbial  
683 fuel cell. *International Journal of Systematic and Evolutionary Microbiology*,  
684 63(PART3), 925–929. <https://doi.org/10.1099/ijs.0.040998-0>

685 Zhao, Y., Feng, C., Wang, Q., Yang, Y., Zhang, Z., Sugiura, N., 2011. Nitrate removal  
686 from groundwater by cooperating heterotrophic with autotrophic denitrification

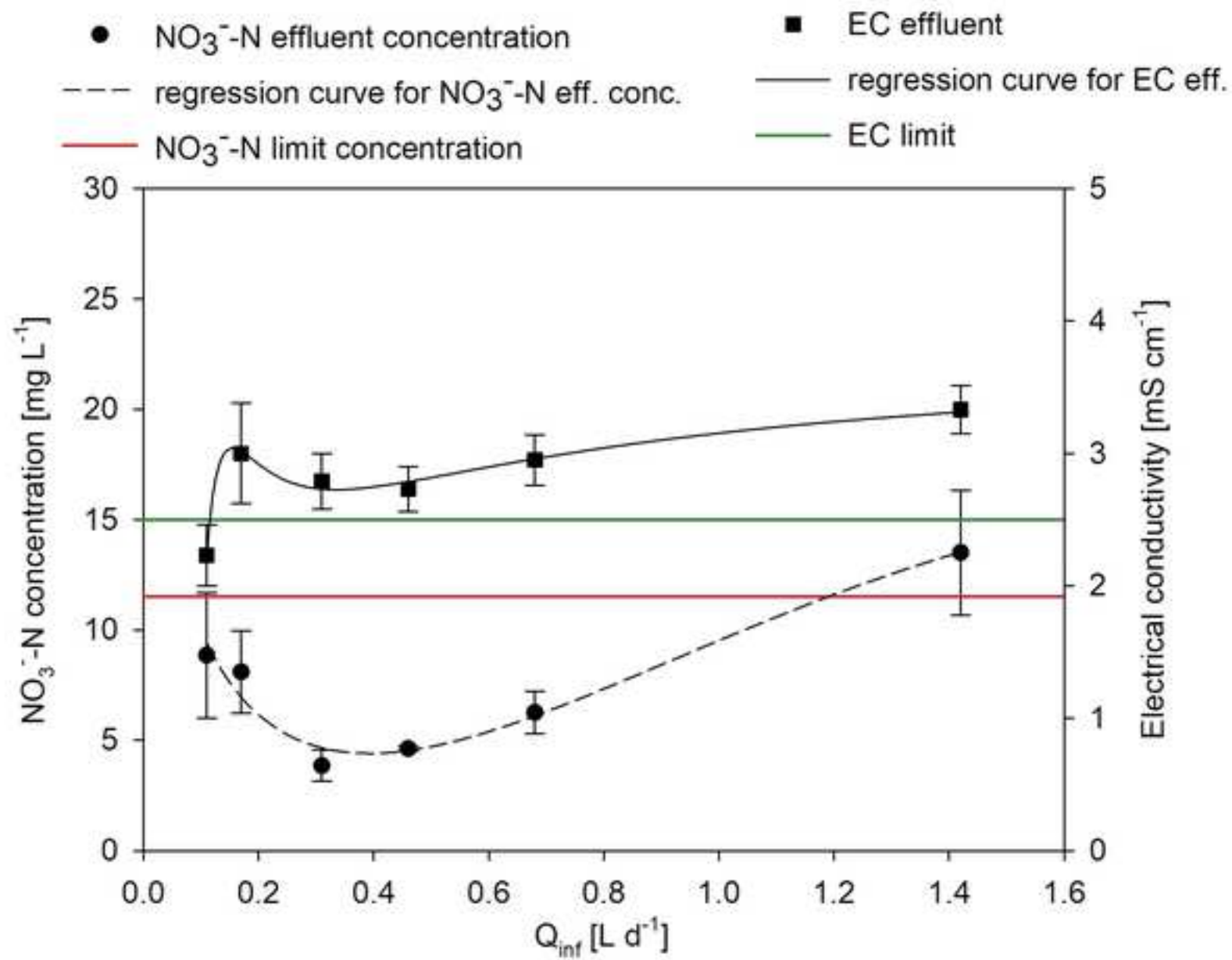
687 in a biofilm–electrode reactor. *J. Hazard. Mater.* 192, 1033–1039.  
688 <https://doi.org/10.1016/j.jhazmat.2011.06.008>

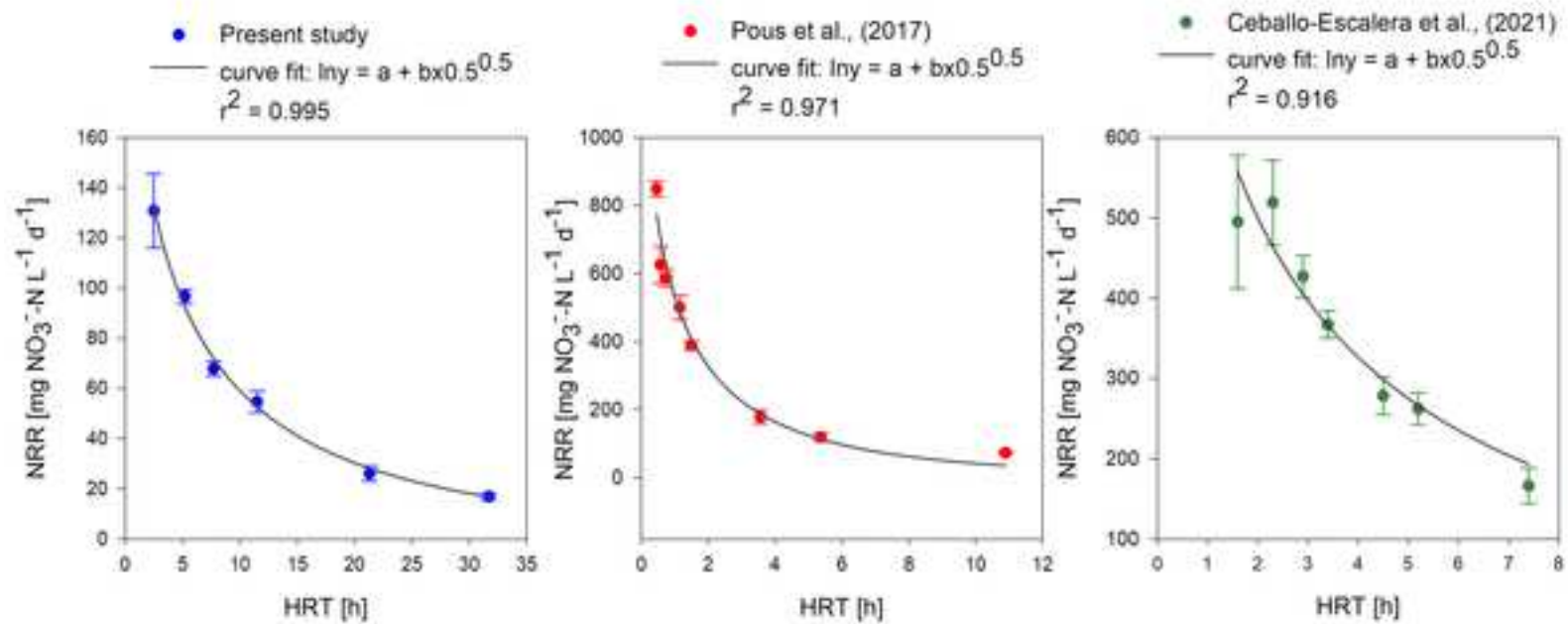
Table 1. Experimental procedure.

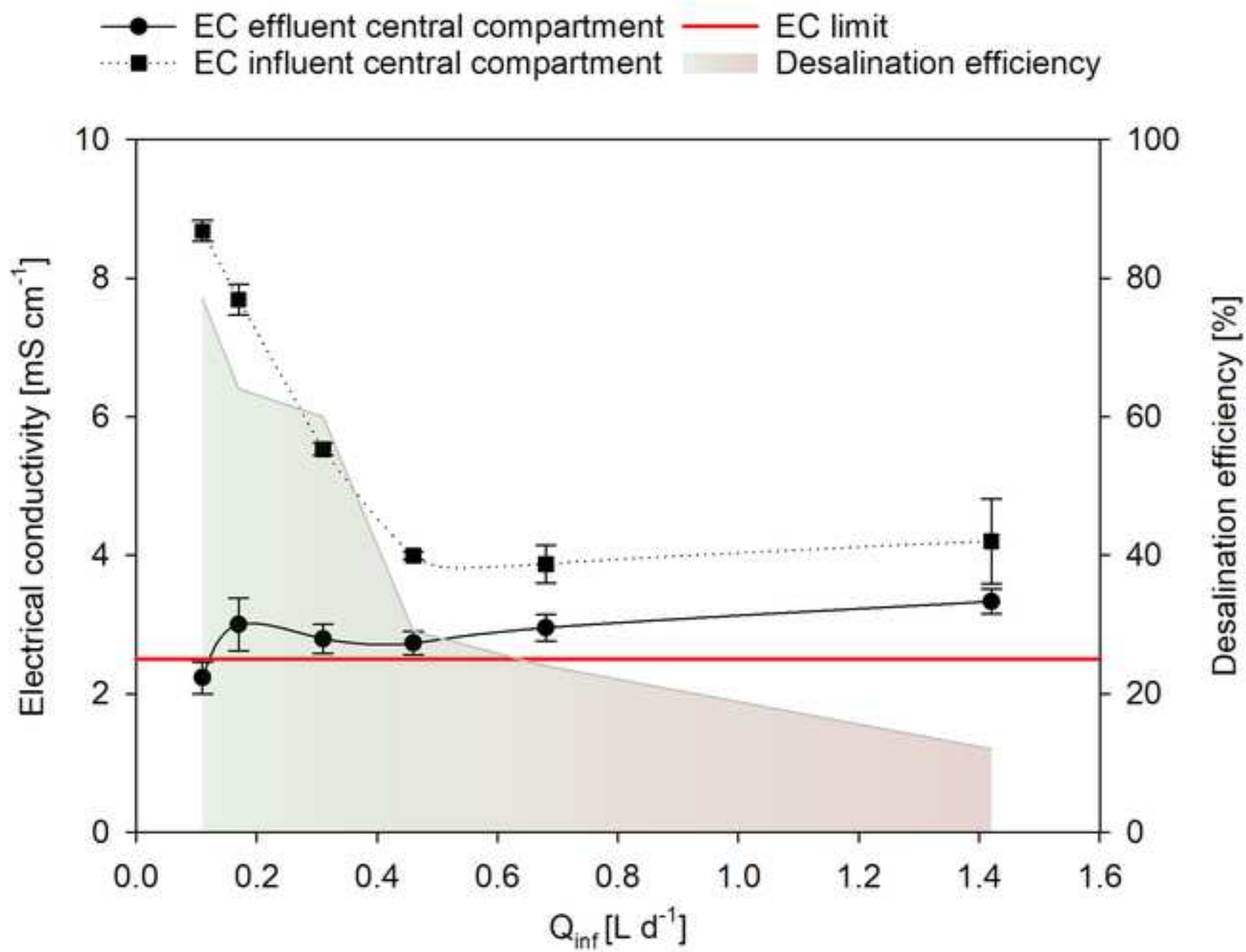
<b>Tests</b>	<b>Influent flowrate [L d<sup>-1</sup>]</b>	<b>HRT Bio-cathode + central compartment [h]</b>	<b>HRT' central compartment [h]</b>	<b>NO<sub>3</sub><sup>-</sup>-N loading rate [mg L<sup>-1</sup> d<sup>-1</sup>]</b>
1	0.11	30.1±2.3	6.7±0.3	23.57±1.84
2	0.17	20.3±1.5	4.5±0.2	35.14±2.39
3	0.31	10.9±0.8	2.4±0.1	62.61±3.90
4	0.46	7.3±0.6	1.6±0.1	82.21±3.07
5	0.68	4.9±0.4	1.1±0.05	125.48±2.98
6	1.42	2.4±0.2	0.5±0.02	261.05±16.07
7	0.68	4.9±0.4	1.1±0.05	130.92±11.27

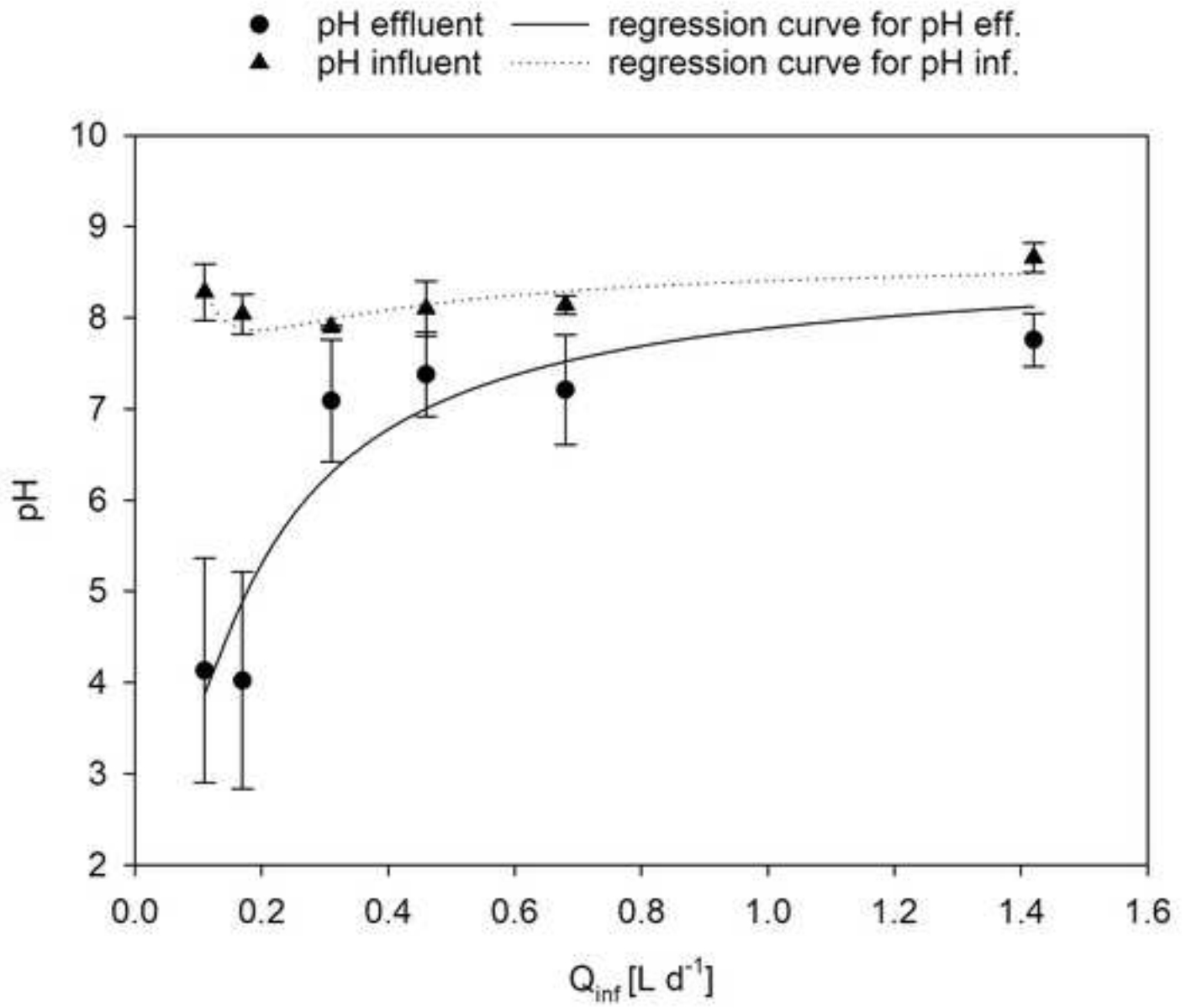


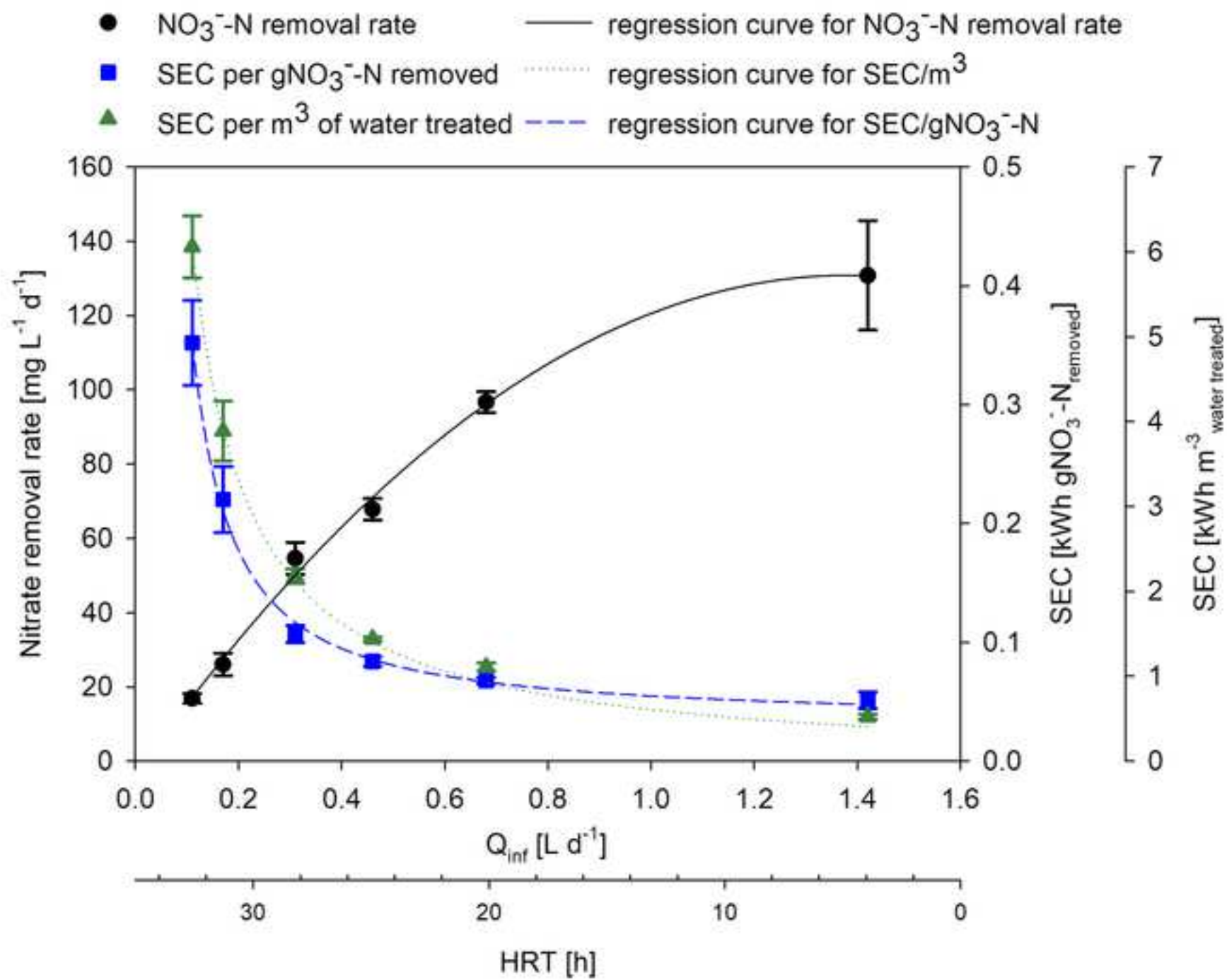


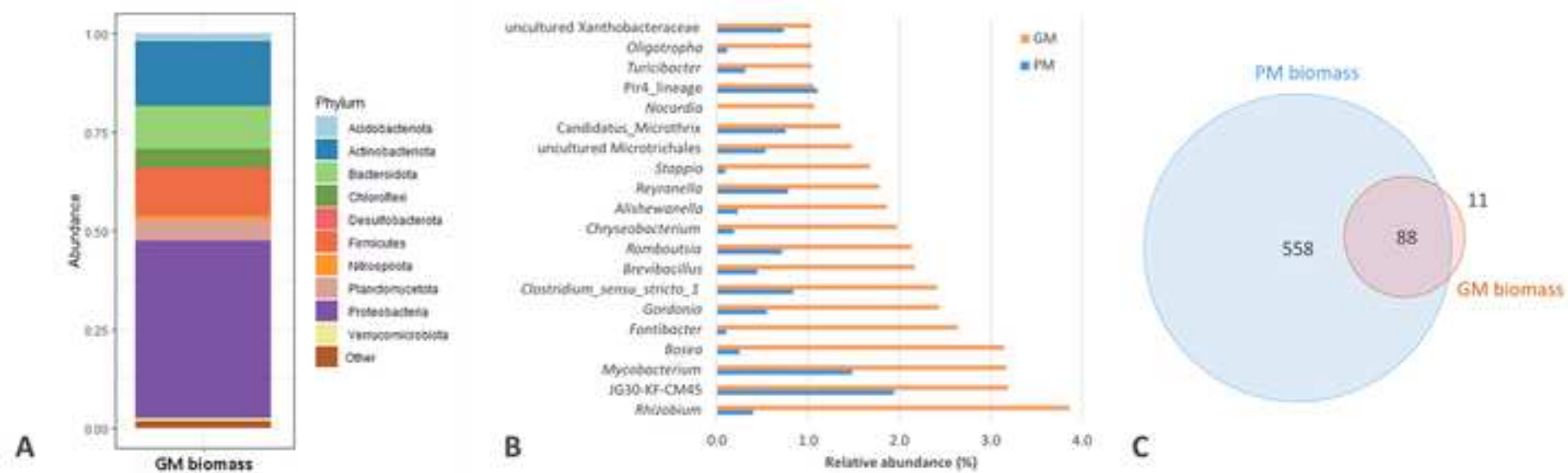


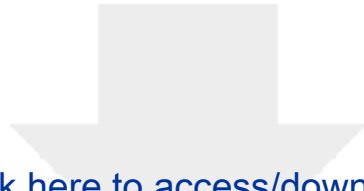








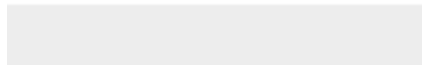




Click here to access/download

**Supplementary Material**

Supplementary material\_STOTEN.pdf



**Declaration of interests**

The authors declare that they have no known competing financial interests or personal relationships that could have appeared to influence the work reported in this paper.

The authors declare the following financial interests/personal relationships which may be considered as potential competing interests:



**Author contribution statement**

The manuscript was written through the contributions of all authors. G. Puggioni: Conceptualisation, Data curation, Investigation, Methodology, Writing – original draft; S. Milia: Conceptualisation, Methodology, Supervision, Funding acquisition, Writing – Review & Editing; V. Unali: Data curation, Investigation, Methodology; R. Ardu: Data curation, Investigation; E. Tamburini: Data curation, Writing - Review & Editing; N. Pous: Conceptualisation, Methodology, Supervision, Writing – Review & Editing; M. D. Balaguer: Conceptualisation, Writing – Review & Editing; S. Puig: Conceptualisation, Methodology, Supervision, Writing – Review & Editing; A. Carucci: Supervision, Funding acquisition, Writing – Review & Editing. All authors have given approval to the final version of the manuscript.